ISTANBUL TECHNICAL UNIVERSITY ★ GRADUATE SCHOOL

QUADROTOR ACTUATOR FAULT DETECTION AND ISOLATION A MODEL BASED APPROACH

M.Sc. THESIS

Muhammed ARSLAN

Department of Aeronautics and Astronautics Engineering

Aeronautics and Astronautics Engineering Program

JUNE 2025

ISTANBUL TECHNICAL UNIVERSITY ★ GRADUATE SCHOOL

QUADROTOR ACTUATOR FAULT DETECTION AND ISOLATION A MODEL BASED APPROACH

M.Sc. THESIS

Muhammed ARSLAN
(511211176)

Department of Aeronautics and Astronautics Engineering

Aeronautics and Astronautics Engineering Program

Thesis Advisor: Prof. Dr. Gökhan INALHAN

JUNE 2025

İSTANBUL TEKNİK ÜNİVERSİTESİ ★ LİSANSÜSTÜ EĞİTİM ENSTİTÜSÜ

DÖNER KANAT AKTÜATÖR ARIZA TESPIT VE IZOLASYON MODEL TABANLI YAKLAŞIM

YÜKSEK LİSANS TEZİ

Muhammed ARSLAN
(511211176)

Uçak ve Uzay Anabilim Dalı

Uçak ve Uzay Mühendislik Program

Tez Danışmanı: Prof. Dr. Gökhan INALHAN

HAZİRAN 2025

Muhammed ARSLAN, a M.Sc. student of ITU Graduate School student ID 511211176 successfully defended the thesis entitled "QUADROTOR ACTUATOR FAULT DETECTION AND ISOLATION A MODEL BASED APPROACH", which he/she prepared after fulfilling the requirements specified in the associated legislations, before the jury whose signatures are below.

Thesis Advisor :	**Prof. Dr. Gökhan INALHAN** Istanbul Technical University	.....
Jury Members :	**Doc. Dr. Barış BAŞPINAR** Istanbul Technical University	.....
	Dr. Mevlüt UZUN Istanbul Technical University	.....
		.....

Date of Submission : **30 May 2025**
Date of Defense : **25 June 2025**

To my father and wife,

FOREWORD

First of all, and before anything, thanks to god for being with us in every moment. Secondly, I would like to dedicate this work to two incredibly important people in my life: my father and my wife.

First, I dedicate this work to my father, whose dreams and hopes for my success have always been a guiding force in my life. Although he is no longer with us, his influence continues to shape my decisions and actions every day. His legacy, wisdom, and love will forever remain in my heart.

I am also profoundly grateful to my wife, whose unwavering support and love have been a constant source of strength throughout my journey. She has not only taken care of our children but has also given me the opportunity and space to dedicate myself to my studies. Her sacrifices and encouragement have been invaluable in enabling me to pursue this academic path, and I could not have reached this point without her.

June 2025

Muhammed ARSLAN
(Aerospace Engineer)

TABLE OF CONTENTS

ABBREVIATIONS

UAV	**:** Unmanned Aerial Vehicle
FDI	**:** Fault Detection and Isolation
FTC	**:** Fault Tolerant Control
qLPV	**:** Quasi Linear Parameter Varying
VTOL	**:** Vertical Take off and Landing
LoE	**:** Loss of Efficiency
RPM	**:** Revolution per Minute

SYMBOLS

m	**:** Mass
I_x, I_y, I_z	**:** Moment of inertia Components
R_{IB}	**:** Directional cosine matrix
ϕ,θ,ψ	**:** Euler velocity
p,q,r	**:** Angular velocity
a	**:** acceleration
u, v	**:** Displacement Vector Components
T	**:** Thrust
g	**:** Gravitational acceleration
ω	**:** Angular velocity
τ_ϕ, τ_θ, τ_ψ	**:** Moment Components
q_0, q_1, q_2 q_3,	**:** Quaternion Components
W	**:** Motor health indicator
t	**:** Time

LIST OF TABLES

LIST OF FIGURES

Page

QUADROTOR ACTUATOR FAULT DETECTION AND ISOLATION
A MODEL BASED APPROACH

SUMMARY

Unmanned Aerial Vehicles (UAVs), particularly quad-rotors, have gained increasing importance across a wide range of civilian and industrial applications due to their maneuverability, vertical take-off and landing (VTOL) capabilities, and mechanical simplicity. However, their inherently nonlinear, unstable, and underactuated dynamics make them highly sensitive to actuator faults, especially those related to the brushless DC motors that directly influence flight control. Any degradation in motor performance, such as loss of effectiveness (LOE), can compromise flight safety and mission success.

This thesis focuses on developing a robust model-based Fault Detection and Isolation (FDI) system capable of detecting and isolating actuator faults in real-time without requiring direct motor feedback. The proposed methodology integrates two complementary observers: a nonlinear Thau observer for estimating system states and detecting deviations in attitude dynamics and a dynamic inversion-based observer that reconstructs actuator behavior from measured accelerations and angular rates. The combination of these two observers enables dual-residual evaluation, enhancing detection sensitivity and fault isolation performance, even under noisy measurements and model uncertainties.

The nonlinear Thau observer is designed using the full Newton-Euler dynamic equations of the quadrotor, avoiding linearization and enhancing estimation accuracy across the entire flight envelope. The dynamic inversion observer provides a secondary set of residuals by comparing estimated motor responses with expected motor behavior. An adaptive thresholding technique is implemented to handle noise and varying flight conditions, while a two-stage magnitude estimation mechanism enables both fast detection and reliable steady-state assessment of fault severity. Finally, a fault-tolerant control allocation strategy is incorporated to compensate for the detected faults using the estimated fault magnitudes.

The complete system was tested in a simulation environment with a realistic quadrotor model. Various fault scenarios, including sudden and progressive LOE faults affecting different motors, were introduced. The results show that the proposed system effectively detects faults within a range of 0.1 to 0.3 seconds from the moment they occur. The fault magnitude was accurately estimated, enabling the controller to adjust thrust using a fault-tolerant control allocation strategy. This allowed the quadrotor to maintain stability and successfully complete its mission, even with partial motor faults. The simulation results validate that the system is capable of detecting both sudden and gradual Loss of Effectiveness (LOE) faults, estimating their magnitude, and ensuring consistent control performance.

Overall, the approach developed in this thesis presents a real-time, lightweight FDI solution that enhances the reliability and safety of quadrotor UAVs, making it suitable for practical application in mission-critical scenarios.

DÖNER KANAT AKTÜATÖR ARIZA TESPIT VE IZOLASYON MODEL TABANLI YAKLAŞIM

ÖZET

İnsansız Hava Araçları (İHA'lar), özellikle quadrotorlar, son yıllarda teknolojik gelişmelerin bir sonucu olarak sivil ve endüstriyel alanlarda büyük bir ivme kazanmıştır. Bu araçlar, manevra kabiliyetleri, dikey kalkış ve iniş (VTOL) yetenekleri ile mekanik sadelikleri sayesinde tarım, güvenlik, lojistik, arama-kurtarma ve hatta film prodüksiyonu gibi çok çeşitli uygulamalarda tercih edilmektedir. Küçük boyutları ve esnek yapıları, quadrotorları hem ticari hem de askeri operasyonlar için cazip hale getirse de, bu sistemlerin doğası gereği doğrusal olmayan, kararsız ve eksik aktüatörlü dinamikleri, uçuş kontrolünü doğrudan etkileyen fırçasız DC motorlardaki arızalara karşı oldukça hassas olmalarını sağlar. Motor performansında meydana gelebilecek herhangi bir bozulma, örneğin etkinlik kaybı (Loss of Effectiveness - LOE), uçuş güvenliğini riske atabilir, görev başarısını tehlikeye sokabilir ve hatta ciddi kazalara yol açabilir. Bu bağlamda, quadrotorların güvenilirliğini ve operasyonel sürekliliğini artırmak için arızaların erken tespiti ve izolasyonu kritik bir öneme sahiptir. Bu tez, bu ihtiyacı karşılamak amacıyla, doğrudan motor geri bildirimi gerektirmeyen, gerçek zamanlı ve sağlam bir model tabanlı Arıza Tespiti ve İzolasyonu (FDI) sistemi geliştirmeyi amaçlamaktadır. Çalışma, quadrotorların küçük ölçekli yapısına uygun, kaynak dostu bir çözüm sunarak, bu araçların hem güvenlik hem de özerklik açısından daha güvenilir hale gelmesine katkıda bulunmayı hedefler. Bu bağlamda, tezimin motivasyonu, hem akademik hem de pratik bir perspektiften, quadrotorların arıza dayanıklılığını artırmak ve bu alandaki literatüre yenilikçi bir katkı sağlamaktır.

Arıza yönetimi sistemleri genellikle üç ana kategoride sınıflandırılır: model tabanlı, veri tabanlı ve hibrit yöntemler. Model tabanlı yaklaşımlar, quadrotorun matematiksel modelini temel alarak arızaları tespit etmeyi amaçlar ve özellikle doğrusal olmayan dinamiklere sahip sistemler için sağlam bir çerçeve sunar. Veri tabanlı yöntemler, yapay sinir ağları ve uzun kısa vadeli bellek (LSTM) ağları gibi makine öğrenimi teknikleriyle büyük veri setlerinden arıza paternlerini çıkararak çalışır, ancak model eksiklikleri ve çevresel belirsizlikler karşısında sınırlı kalabilir. Hibrit yöntemler ise bu iki yaklaşımın avantajlarını birleştirerek daha kapsamlı çözümler sunmayı hedefler, fakat karmaşıklıkları nedeniyle gerçek zamanlı uygulamalarda bazı zorluklar doğurabilir.

Bu tezde benimsenen yöntem, model tabanlı bir stratejiye dayanır ve iki tamamlayıcı gözlemciyi birleştirir: doğrusal olmayan Thau gözlemcisi ve dinamik tersine çevirme tabanlı bir aktüatör residüel gözlemcisi. Bu yaklaşım, literatürdeki doğrusal gözlemci sınırlamalarını aşarak, quadrotorun tam dinamik modelini kullanır ve adaptif eşikleme ile gürültüye karşı robustness sağlar. Ayrıca, arıza büyüklüğünü tahmin ederek hata toleransı kontrol tahsisine entegre eden bir mekanizma geliştirilmiştir. Bu, önceki

çalışmalardan farklı olarak, hem hızlı tespit hem de uzun vadeli izleme yeteneği sunar. Yöntem, kaynak kısıtlamalı platformlar için optimize edilerek, literatüre pratik ve ölçeklenebilir bir katkı sağlamayı amaçlar.

Çalışmada, 2.3 kg kütleli gerçekçi bir quadrotor modeli MATLAB/Simulink ortamında geliştirilmiştir. Bu model, quadrotorun fiziksel parametrelerini (örneğin, kütle merkezi, atalet momenti) ve motor özelliklerini (itki katsayıları, tork ilişkileri) dikkate alarak, gerçek dünya koşullarını yansıtmaktadır. Quadrotor, dört simetrik rotoru ile lift ve kontrolü sağlayan bir yapıya sahiptir; bu rotorlar, dikey hareketi sağlarken, açısal momentum farklarıyla tutum kontrolü gerçekleştirir. Dinamik model, Newton-Euler formalism kullanılarak türetilmiş ve 6 serbestlik derecesine sahip tam bir doğrusal olmayan model olarak formüle edilmiştir.

Translasyonel dinamikler, motorların ürettiği itki kuvveti, yerçekimi ve dış kuvvetlerin (örneğin rüzgar) etkisini dikkate alarak, atalet çerçevesindeki ivmeleri hesaplar. Rotasyonel dinamikler ise, motor torkları ve açısal hızlar üzerinden tutum değişimlerini tanımlar. Aktüatör sağlığı, her motor için W_i parametresiyle modellenmiştir; $W_i = 1$ tam sağlık, $W_i < 1$ ise etkinlik kaybını gösterir. Bu model, ani ve kademeli LOE arızalarını simüle etmek için geliştirilmiş ve kontrolör ile FDI sisteminin entegrasyonuna temel oluşturmuştur. Modelin doğrulanması, literatürdeki standart test verileriyle karşılaştırılarak gerçekleştirilmiş ve bu, simülasyonların güvenilirliğini artırmıştır.

Geliştirilen FDI sistemi iki temel yapıdan oluşmaktadır:

- Thau Gözlemcisi (Thau Observer): Bu yapı, quadrotorun tam dinamik modeline dayanarak sistem durumlarını (konum, hız, tutum) tahmin eder ve doğrusallaştırma gerektirmeden tüm uçuş koşullarına uyum sağlar. Bu gözlemci, başlangıçta silahsız (disarm) modda ölçülen verilerle sürekli senkronize edilir; kalkış moduna geçtiğinde ise tek bir ölçümle initialize edilerek bağımsız izlemeye başlar. Tutum residüelleri (roll, pitch, yaw), motor arızalarının daha hızlı etkilediği bu parametreler üzerinden değerlendirilir.

- Dinamik Tersleme Temelli Tamamlayıcı Gözlemci (Dynamic Inversion Based Observer): Bu gözlemci, ölçülen ivme ve açısal hız verilerinden aktüatör davranışını yeniden yapılandırır ve ikinci bir residüel seti oluşturur. Bu, arıza izolasyonunu güçlendirir ve motor sağlığı tahminlerini iyileştirir. Adaptif eşikleme tekniği, nominal çalışma verilerinin istatistiksel özelliklerine dayanarak eşik değerlerini dinamik olarak ayarlar ve yanlış alarmları önler. İki aşamalı büyüklük tahmin mekanizması, arızanın başlangıcını hızlıca tespit eder (ilk aşama) ve ardından motor bozulmasının zamanla nasıl ilerlediğini izler (ikinci aşama). Bu mekanizma, motor devir sayısına (RPM) dayalı bir gözlemciyle desteklenerek, kademeli arızalarda hassasiyet sağlar.

Bu çift gözlemci yapısı sayesinde, sistem hem arıza tespiti hem de arızanın türü (ani ya da kademeli) ve şiddeti hakkında bilgi sağlayabilir. Ayrıca sistemin en büyük avantajlarından biri, doğrudan aktüatör geri beslemesi gerektirmeyen yapısıdır. Bu sayede ağırlık ve karmaşıklık bakımından sınırlı olan İHA sistemlerine kolayca entegre edilebilir.

Tespit edilen arızaları telafi etmek için, bir hata toleransı kontrol tahsis stratejisi geliştirilmiştir. Bu strateji, her motorun etkinliğini yansıtan bir sağlık matrisi (W_c) kullanarak itkiyi yeniden dağıtır. Ani veya kademeli LOE arızalarında, bu sistem motor komutlarını gerçek zamanlı olarak ayarlayarak quadrotorun istikrarını korur.

Simülasyonlar , MATLAB/Simulink ortamında 60 ve 120 saniyelik simülasyonlarla test edilmiştir. Başlangıç koşulları, quadrotorun yerde sıfır hız ve açıyla durduğu tipik bir kalkış senaryosunu yansıtmıştır. Thau gözlemcisi, kalkış modunda ölçülen verilerle initialize edilir ve residüel üretimi yerde modda başlayıp kalkışla aktif hale gelir. Adaptif eşik değerleri ise yerde hesaplanarak uçuş sırasında kullanılır.

Tezde önerilen FDI sisteminin test etmek amacıyla çeşit test senaryolar uygulanmıştır. Bu senaryolar;

1. Nominal çalışma durumu (hiçbir arızanın bulunmadığı durum),
2. Ani etkinlik kaybı (Sudden Loss-of-Effectiveness, LoE),
3. Kademeli etkinlik kaybı (Gradual LoE),

olarak sınıflandırılmıştır. İkinci ve üçüncü senaryolarda, dört motorun her biri için ayrı ayrı uygulanmıştır. Ayrıca her test iki farklı koşul altında gerçekleştirilmiştir:

1. Normal koşullar: düşük seviye sensör gürültüsü ve rüzgar etkisi olmayan durumlar.
2. Dış bozucular altında koşullar: 3 m/s'lik sabit rüzgar, 2 m/s ani rüzgar darbeleri ve sensör gürültüsü.Gürültü ($\pm 1^\circ$) duruş açılara ve açısal hızlara uygulanmıştır

Ayrıca model parametrelere hata payı eklenmiştir ;

1. Atalet momentler yüzde 15 hata payı eklenmiştir,
2. autopilottaki motor model parameterleri modelden farklı tutulmuştur,

Nominal koşullarda, residüeller eşik içinde kalarak yanlış alarmların olmadığını doğrulamıştır; izleme hatası minimaldir ve motor sağlık göstergeleri birliğe yakın kalmıştır. Ani LOE senaryosunda, sistem arızayı 0.1-0.15 saniye içinde tespit etmiş, tutum residüelleri (özellikle roll ve pitch) keskin artışlar göstermiş ve dinamik tersine çevirme gözlemcisi motor sağlığı tahminlerinde tutarlı düşüşler sergilemiştir. Kontrolör, itkiyi yeniden tahsis ederek istikrarı korumuş ve quadrotor görevini tamamlamıştır. Kademeli LOE'de, Thau gözlemcisi residüellerle arızayı 0.1-0.2 saniye içinde yakalamış, tamamlayıcı gözlemci ise hata miktari etkin bir şekilde takıp etmiştir. Yüzde 10'dan 40'a uzanan bozulmayı düşük hata miktar ile takip yaklamıştır. Tüm testlerde hiçbir yanlış tespit görülmemiştir ve residüeller eşik değerler için tutulmuştur.

Özet olarak, önerilen FDI sisteminin ani ve kademeli LOE arızalarını güvenilir bir şekilde tespit ettiğini, hata büyüklüklerini doğru tahmin ettiğini ve stabil kontrol performansını sürdürdüğünü kanıtlamaktadır. Sistemin gürültü, rüzgar ve model hatalarına karşı gösterdiği dayanıklılık, onu küçük ölçekli quadrotorlar için gerçek zamanlı bir çözüm haline getirmektedir. Bu çalışma, literatüre pratik ve ölçeklenebilir bir katkı sunarken, gelecekte çoklu arıza tespiti ve donanım entegrasyonu gibi alanlarda geliştirilmeye açıktır.

1. INTRODUCTION

Unmanned Aerial Vehicles (UAVs), particularly quad-rotors, are increasingly integrated into various fields, including surveillance, agriculture, inspection, and delivery services, due to their vertical take-off and landing (VTOL) capabilities and mechanical simplicity. The design of the quad-rotors consists of a four-rotor design, where each rotor is driven by a DC motor, creating lift and control. This Design gives quad-rotors better maneuverability compared to traditional helicopters, as they can hover, move in any direction, and change altitude easily.

Despite these advantages, quad-rotors are inherently sensitive systems characterized by nonlinear dynamics and instability. The quad-rotor systems are generally considered an unstable system since it is underactuated, which means that they have four control surfaces while trying to control a six- degree-of-freedom system. Any faults or failures in quad-rotor motors can lead rapidly to degraded control, unstable flight conditions, or catastrophic system failure. Motor faults may occur due to various reasons, such as mechanical wear, electrical malfunctions, or environmental influences such as debris or adverse weather conditions [2] [3].

Considering how serious actuator faults can be, creating and putting into action effective Fault Detection and Isolation (FDI) systems feels like a must. These systems are key to spotting problems quickly and figuring out where they're coming from, giving us a chance to step in with fixes or switch on fault-tolerant controls to keep everything steady and avoid major mishaps. Having solid FDI methods in place significantly enhances the safety and dependability of operations, enabling UAVs to carry out vital missions even when things go wrong.

The quad-rotor motors are prone to more than one type of fault, each with its own physical origin and characteristic flight signature. Understanding these categories is crucial for designing appropriate FDI schemes.

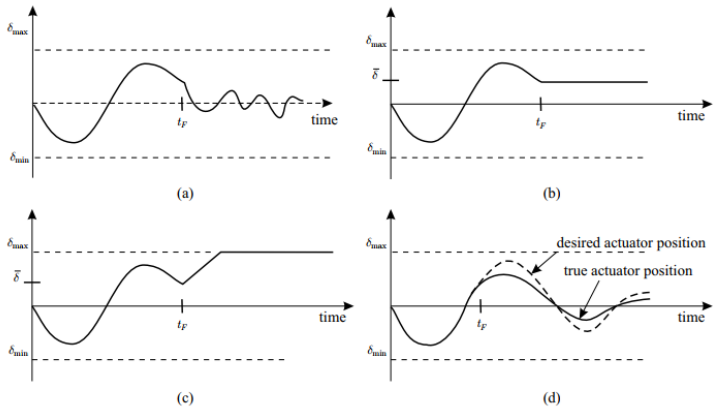

Figure 1.1 : Actuator common fault types: (a) floating around trim; (b) locked-in-place; (c) hard-over; and (d) loss of effectiveness [1]

- **Partial Loss of Effectiveness (LoE):** A gradual or sudden reduction in thrust output, often caused by motor winding degradation, bearing wear, or increased electrical resistance.

- **Total Loss of Effectiveness (LoE):** A total loss- failure in thrust output. Usually caused by Open-circuit or short-circuit conditions in the stator windings, alter the torque constants, or cause thermal shutdown. Often presents initially as Low Energy, then progresses to total failure.

- **Lock-in-Place Faults:** The motor cannot drive to full thrust (stuck-high) or zero thrust (stuck-low) if it exceeds a given speed threshold, regardless of the command. These abrupt faults typically stem from ESC failures or signal shorts, resulting in sudden, large attitude excursions.

- **Intermittent Faults:** Unpredictable dropouts or flickers in thrust due to loose wiring, overheating cut-outs, or controller glitches. These are challenging for FDI because fault signatures appear and vanish erratically.

Each fault type presents unique challenges and demands specific strategies within the FDI framework to effectively manage and mitigate its impact on the UAV's performance and stability.

This work focuses on developing a fault detection and isolation algorithm (FDI) that addresses loss of effectiveness (LOF) faults, isolates the faults, and subsequently applies a fault tolerance control allocation to mitigate partial loss of effectiveness.

1.1 Literature Review

Fault management systems generally proceed through three main stages: fault detection (FD), fault isolation (FI), and fault tolerance (FT)—each building upon the last. Fault detection is the process of recognizing that the system's behavior has deviated from its expected or nominal operation, typically by monitoring the system's behavior and detecting residuals or statistical indicators. Once a fault is detected, fault isolation identifies which component or subsystem is responsible, narrowing the problem to a specific sensor, actuator, or processing unit. Finally, fault-tolerance refers to the system's ability to continue safe and effective operation despite the identified fault, often by reconfiguring control laws or redistributing commands among remaining healthy components. Whereas detection only flags "something is wrong" and isolation pins down "where it is," fault-tolerance ensures "what to do" so the mission can proceed without catastrophic failure [4]. As mentioned earlier in the previous section, this work focuses on fault detection and isolation with a tolerance mechanism in the control allocation that can deal with partial LoE. [5] [6]

The existing fault detection methods in the literature can be categorized into three primary methods/approaches as shown in Figure **??**. Model-based approaches, data-driven approaches, and hybrid approaches. Model-based techniques utilize system dynamics and mathematical models to detect anomalies by comparing predicted outputs to actual measurements. On the other hand, Data-driven approaches rely on flight data logs and machine learning algorithms to recognize patterns indicative of faults or on the feedback measurements from sensors on actuators to determine the faults. Hybrid methods combine aspects of both model-based and data-driven techniques, aiming to leverage the strengths of each while mitigating their limitations.

Various model-based approaches have been explicitly proposed for quad-rotors, capitalizing on their mathematical models to achieve accurate fault detection. [7] [8]

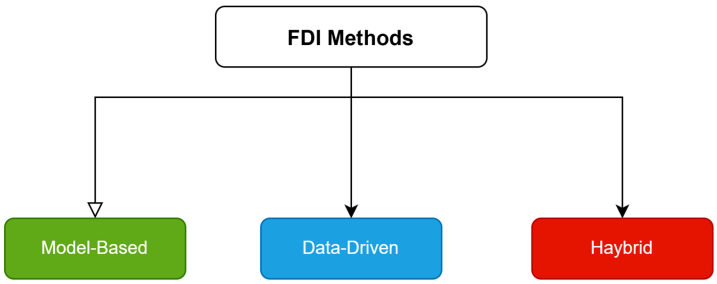

Figure 1.2 : FDI methods classification.

developed a nonlinear observer to monitor quad-rotor dynamics and effectively detect motor faults through residual generation. [9] introduces an actuator fault detection and isolation (FDI) method for a quadrotor UAV, modeled as a qLPV system. They developed a robust H_∞ observer, which facilitates fault detection and isolation by identifying faulty actuators through a simplified model of the quadrotor. Different versions of the Kalman filter are also being used to estimate the faults in quad-rotors [1].

Data-driven approaches are benefiting from several algorithm, such as neural networks, reinforcement learning, statistical methods, as well as measurement feedback. In [10], a comprehensive system is introduced for detecting errors, diagnosing faults, and recovering a coaxial octocopter based on the measurement data. They utilize the speed feedback of the motor's electronic speed controller (ESC) to detect the faults. After fault detection, they adjust the control allocation matrix and differentiate between motor failures and propeller losses.

Hybrid approaches combine both model-based and data-driven methods, which get usees of the strengths of each to improve fault detection and isolation. These methods are particularly effective in real-time applications where system models may be incomplete, and environmental conditions are unpredictable. In [11], A combination of dynamic and data-driven models is employed to generate training data, which is then used by a deep neural network, specifically the long short-term memory (LSTM) network, to estimate the torque and thrust of faulty propellers.

1.2 Hypothesis and Contribution

1.2.1 Hypothesis

This thesis is based on the hypothesis that combining a nonlinear state observer with a dynamic inversion-based actuator residual observer enables effective detection, isolation, and magnitude estimation of actuator faults in quadrotor UAVs. It is assumed that, even in the absence of direct actuator feedback, such a model-based approach can achieve timely and reliable fault diagnosis under disturbances, noise, and model uncertainties. Furthermore, it is hypothesized that this dual-residual framework can support fault-tolerant control by providing actionable estimates of motor effectiveness loss.

This thesis is built on the hypothesis that integrating a nonlinear observer based on the full dynamics of the quadrotor with a dynamic inversion-based actuator residual observer allows for effective, real-time detection and isolation of actuator faults—specifically loss-of-effectiveness (LOE) faults—without requiring actuator feedback. It is assumed that such an approach can:

- Accurately estimate system states and detect actuator faults within a short time after fault fault,
- Distinguish between different motor faults (e.g., partial vs. total LOE),
- Remain robust under measurement noise, wind disturbances, and deviations in model parameters.

Furthermore, it is hypothesized that the proposed adaptive dual-observer strategy can do fast detection as well as estimation of fault magnitude, which can be directly used in fault-tolerant control reallocation mechanisms.

1.2.2 Contribution

The potential contributions of this thesis are summarized below:

1. **Enhancement of the Thau observer** by formulating it based on nonlinear quadrotor dynamics, making it suitable for full-envelope estimation without relying on linearization.

2. **Development of an actuator health estimation scheme** using a dynamic inversion-based residual generator, which tracks the evolution of actuator degradation using an RPM-based observer. A dual-phase logic ensures both rapid response and steady-state accuracy. Improving fault type identification and fault magnitude estimation.

3. **Increasing robustness against disturbances, noises, and deviation in model parameters** , design of a dual-residual FDI framework increasing sensitivity, robustness, and reducing false alarms.

4. **Integration of a fault-tolerant control allocation method**, which adjusts motor commands in real-time based on the estimated loss of effectiveness, allowing continued stable flight even under partial motor failure.

1.3 Thesis Outline

The thesis is structured into six chapters, each addressing a specific component of the research, beginning with the mathematical modeling of the quad-rotor and progressing to the implementation and validation of the proposed Fault Detection and Isolation (FDI) system.

Chapter 2: Quadrotor Dynamics and Mathematical Modeling

This chapter contains a description of the quadrotor UAV platform and its underlying physics. It begins by describing the basic configuration and components of the quadrotor, including its lift layout and reference coordinate frames. The chapter then formulates the complete nonlinear dynamic model of the system using Newton-Euler

formalism. Translational and rotational equations of motion are derived to capture the 6-degree-of-freedom dynamics. Additionally, the actuator and propeller model, including the thrust and torque generation mechanisms of the motors, is discussed. This chapter provides the mathematical foundation upon which the control system and fault detection algorithms are later developed.

Chapter 3: Control Strategy

This chapter outlines the control architecture used to stabilize and navigate the quadrotor. The cascaded dynamic inversion control approach is explained, as well as the control allocation of desired moments to motor commands is also presented.

Chapter 4: Fault Detection and Isolation System

This chapter introduces the core contribution of the thesis: the development and implementation of a fault detection and isolation system for quadrotor actuator faults. It begins by explaining the design of the nonlinear Thau observer, then introduces a complementary fault detection module based on dynamic inversion. Then, the residual evaluation and fault isolation mechanism are explained. Finally, the logic for the tolerated control allocation is presented.

Chapter 5: Simulation and Results

This chapter presents the simulation environment, fault test scenarios, and results used to validate the proposed control and fault detection systems.

Chapter 6: Conclusion

The last chapter contains the thesis's main findings and contributions. It acknowledges the limitations of current work and suggests directions for future research, including real-time implementation, integration with fault-tolerant control, and extension to multi-fault scenarios.

2. QUADROTOR DYNAMICS AND MATHEMATICAL MODELING

Quad-rotors, also known as quad-copters, are a class of Unmanned Aerial Vehicles (UAVs) that utilize four rotors arranged symmetrically to achieve lift and control. Their mechanical simplicity, vertical take-off and landing (VTOL) capability, and agile maneuverability make them suitable for a wide range of applications, from civilian tasks like aerial surveying and inspection to complex missions in defense and research. Unlike fixed-wing UAVs, quad-rotors can hover in place, perform vertical climbs, and execute complex trajectory maneuvers in confined environments.

Several physical configurations exist for quad-rotors, with the most common being the "X" and "+" configurations, as shown in Figure 2.1. In the "+" configuration, one rotor aligns with the forward direction of flight, while the "X" configuration orients the rotors diagonally relative to the body axes. The "X" configuration is particularly advantageous for trajectory tracking and agile maneuvering since the thrust direction aligns better with the desired motion commands as well as each degree of freedom can be controlled by two motors, so in case of motor fault, another motor will be available to control the motion by the other motor. In this work, an "X" configuration quadrotor platform is adopted, equipped with four identical brushless DC motors and electronic speed controllers. The total mass of the platform is approximately 2.3 kg, including battery and payload, and it is assumed to have a rigid and symmetric structure. The main physical parameters of the platform used in this thesis are summarized in Table 2.1:

Table 2.1 : Platform physical parameters.

Parameter	Value	Description
m	2.3 kg	Total mass includes frame, battery, and payload
I_{xx}	0.0088 kg·m^2	Moment of Inertia around x-axis
I_{yy}	0.0125 kg·m^2	Moment of Inertia around y-axis
I_{zz}	0.0122 kg·m^2	Moment of Inertia around z-axis

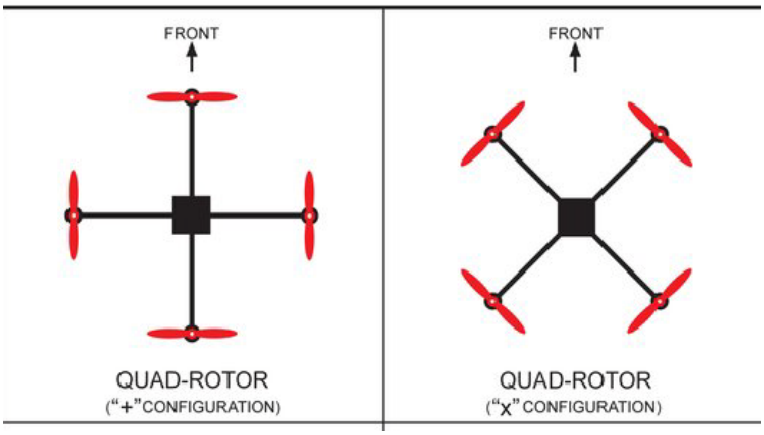

Figure 2.1 : Quad-rotor Configurations.

The overall proposed non-linear mathematical model structure is illustrated in Figure 2.2

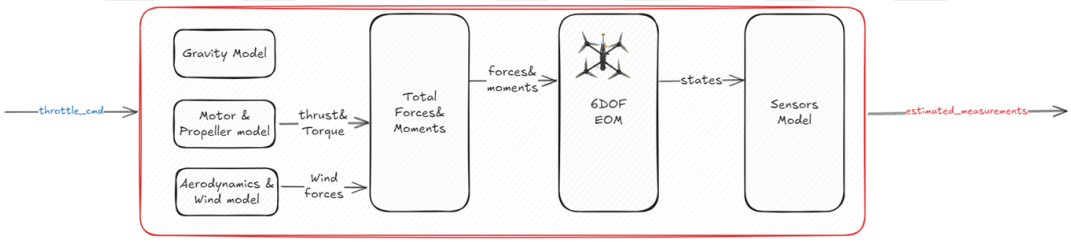

Figure 2.2 : Non-linear model structure.

As illustrated in Figure 2.2, the proposed non-linear aircraft model consists of three main sub-models :

1. 6DOF equation of motion model.
2. Actuator model.
3. Aerodynamic and wind model.

In order to define the dynamic and physical models for the quad-rotors, the frames used to describe the motion have to be mentioned. There are many coordinate frames to describe the aircraft motion, but the most common ones and the ones that will be used in this work are:

1. Inertial Frame (Earth Frame): A fixed frame usually denoted as $I = x_I, y_I, z_I$, with z_I pointing upward. It is used to express the vehicle's position and orientation relative to the global Earth orientation.

2. Body Frame: A moving frame attached to the center of mass of the quad-rotor, denoted as $B = x_B, y_B, z_B$, where x_B points forward, y_B to the right, and z_B downward.

The transformation between these frames is achieved using a Direction Cosine Matrix (DCM), derived from the Euler angles (roll ϕ, pitch θ, and yaw ψ) or using quaternions for better numerical stability in 3D rotations. The DCM that maps body-frame vectors to the inertial frame is given by:

$$R_{IB} = R_\phi R_\theta R_\psi \tag{2.1}$$

$$R_{IB} = \begin{bmatrix} \cos\theta\cos\psi & \cos\theta\sin\psi & -\sin\theta \\ \sin\phi\sin\theta\cos\psi - \cos\phi\sin\psi & \sin\phi\sin\theta\sin\psi + \cos\phi\cos\psi & \sin\phi\cos\theta \\ \cos\phi\sin\theta\cos\psi + \sin\phi\sin\psi & \cos\phi\sin\theta\sin\psi - \sin\phi\cos\psi & \cos\phi\cos\theta \end{bmatrix} \tag{2.2}$$

This rotation matrix R_{IB} is used to convert vectors from the body frame to the inertial frame as follows:

$$\mathbf{I} = R_{IB} \cdot \mathbf{B} \tag{2.3}$$

where $\mathbf{I}$ is a vector expressed in the body frame and $\mathbf{B}$ is the corresponding vector in the inertial frame.

2.1 Equation of Motion

The dynamic model of a quad-rotor includes translational and rotational motion. In this work, the motion was described using a Newtonian approach. The orientation modeling was done based on quaternion representation, which avoids singularities (gimbal lock) and improves numerical stability, making it more suitable for extended simulations and maneuvering.

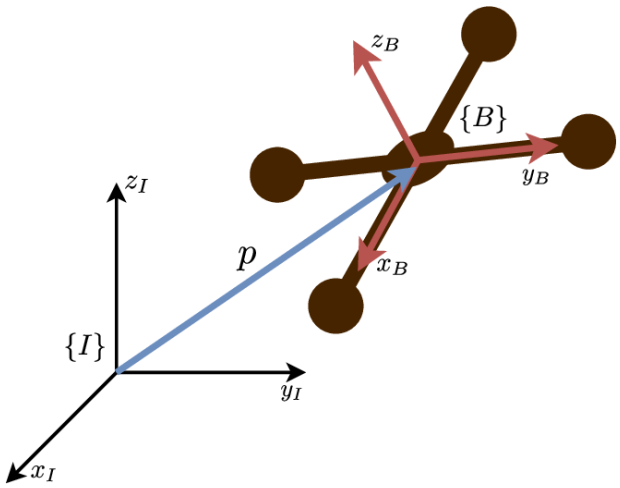

Figure 2.3 : Quad-rotor Frames.

2.1.1 Translational dynamics

Newton's Second Law governs the translational motion of the quadrotor in the inertial frame:

$$\mathbf{F} = m \cdot \mathbf{a} \tag{2.4}$$

$$a = \ddot{\mathbf{x}}_E \tag{2.5}$$

Where $\ddot{x}$ is the translational acceleration of the center of mass in the inertial frame.

For the quadrotor, the forces acting on the system are primarily **thrust** from the motors, **gravity**, and the **external forces** such as the wind or gust. The thrust vector is assumed to be aligned with the body frame, and the total force is the sum of the thrust force, the gravitational force, and external forces:

$$F_{total} = R_{BI} \begin{bmatrix} 0 \\ 0 \\ T \end{bmatrix} - \begin{bmatrix} 0 \\ 0 \\ mg \end{bmatrix} + \begin{bmatrix} Fx_{ext} \\ Fy_{ext} \\ Fz_{ext} \end{bmatrix} \tag{2.6}$$

The total translational acceleration in the inertial frame is given by:

$$\ddot{\mathbf{x}}_E = \frac{F_{total}}{m} \tag{2.7}$$

Where:

- m is the mass of the quadrotor,
- R_{BI} is the transformation matrix from body to inertial frame,
- T is the motor's thrust force acting on the quadrotor body,
- g is the gravity force acting on the inertial frame

2.1.2 Rotational dynamics

To describe the rotational dynamics of the quad-rotor, the total moment applied to the body should be

$$I\dot{\omega} + \omega \times (I\omega) = \tau \tag{2.8}$$

where I is the inertia tensor of the quadrotor, assumed diagonal due to symmetry

$$I = \text{diag}(I_x, I_y, I_z) \tag{2.9}$$

ω is the angular velocity vector expressed in the body frame around the roll, pitch, and yaw axes, respectively

$$\omega = [p \quad q \quad r]^T \tag{2.10}$$

τ is the vector of control torques generated by the motor thrust forces.

$$\tau = [\tau_\phi \quad \tau_\theta \quad \tau_\psi]^T \tag{2.11}$$

expanding the main equation 2.8 the component of the angular accelerations will be

$$\dot{p} = \frac{\tau_\phi - (I_z - I_y)qr}{I_x} \tag{2.12}$$

$$\dot{q} = \frac{\tau_\theta - (I_x - I_z)pr}{I_y} \tag{2.13}$$

$$\dot{r} = \frac{\tau_\psi - (I_y - I_x)pq}{I_z} \tag{2.14}$$

There are two ways of representation to describe the quad-rotor's rotational dynamics: quaternions and Euler angles representation. In this mathematical model, quaternions are adopted due to their numerical stability and avoidance of singularities.

A quaternion is represented as:

$$q = \begin{bmatrix} q_0 \\ q_1 \\ q_2 \\ q_3 \end{bmatrix} \tag{2.15}$$

Which satisfies the normalization constraint:

$$q_0^2 + q_1^2 + q_2^2 + q_3^2 = 1 \tag{2.16}$$

The angular velocity vector ($\omega = [p \quad q \quad r]^T$) relates to the quaternion derivative by:

$$\dot{q} = \frac{1}{2} \begin{bmatrix} 0 & -p & -q & -r \\ p & 0 & r & -q \\ q & -r & 0 & p \\ r & q & -p & 0 \end{bmatrix} q \tag{2.17}$$

The quaternion vector can be calculated by integrating the quaternion rate, and then Euler angles can be extracted from quaternions through the following equations:

$$\phi = \text{atan2}\left(2(q_0 q_1 + q_2 q_3), 1 - 2(q_1^2 + q_2^2)\right) \tag{2.18}$$

$$\theta = \text{asin}\left(2(q_0 q_2 - q_3 q_1)\right) \tag{2.19}$$

$$\psi = \text{atan2}\left(2(q_0 q_3 + q_1 q_2), 1 - 2(q_2^2 + q_3^2)\right) \tag{2.20}$$

2.2 Actuator Model

Each motor in the quadrotor contributes both a vertical thrust and a torque. The total thrust and moments generated by the four rotors are mapped to the body forces and moments using a predefined allocation matrix.

Assuming the rotor numbering follows the standard X-configuration as (Figure 2.4):

- Motor 1: Front Left (CW)
- Motor 2: Front Right (CCW)
- Motor 3: Rear Right (CW)
- Motor 4: Rear Left (CCW)

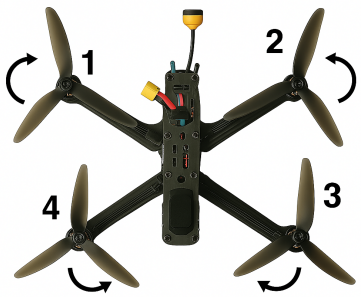

Figure 2.4 : Motor rotation directions.

The motor input is initially derived from the throttle command signal. The throttle command is transferred to the motor angular velocity command RPM using a lookup table from the motor and propeller test data. This command is then processed through a first-order transfer function to simulate the internal motor dynamics and provide a realistic motor angular velocity response. The transfer function can be expressed as:

$$\omega_{act} = \omega_{cmd} - \tau_m \cdot \dot{\omega}_{act} \tag{2.21}$$

where $\omega_{cmd,i}$ is the commanded angular velocity for motor i, ω_i is the actual motor speed, and τ_m is the motor time constant. There is a direct relationship between the motor angular speed and motor thrust, as well as motor torque. The total thrust and torques generated by the motors can be modeled as:

$$\begin{bmatrix} T \\ \tau_\phi \\ \tau_\theta \\ \tau_\psi \end{bmatrix} = \begin{bmatrix} k_t & k_t & k_t & k_t \\ lk_t & -l \cdot k_t & -lk_t & l \cdot k_t \\ l \cdot k_t & l \cdot k_t & -l \cdot k_t & -l \cdot k_t \\ -d & d & -d & d \end{bmatrix} \begin{bmatrix} W_1 \omega_1^2 \\ W_2 \omega_2^2 \\ W_3 \omega_3^2 \\ W_4 \omega_4^2 \end{bmatrix} \tag{2.22}$$

Where:

- k_t is the thrust coefficient.
- d is the torque coefficient.
- l is the arm length from the center of mass to the motor.
- ω_i is the angular speed of motor i.
- W_i is the motor health of motor i.

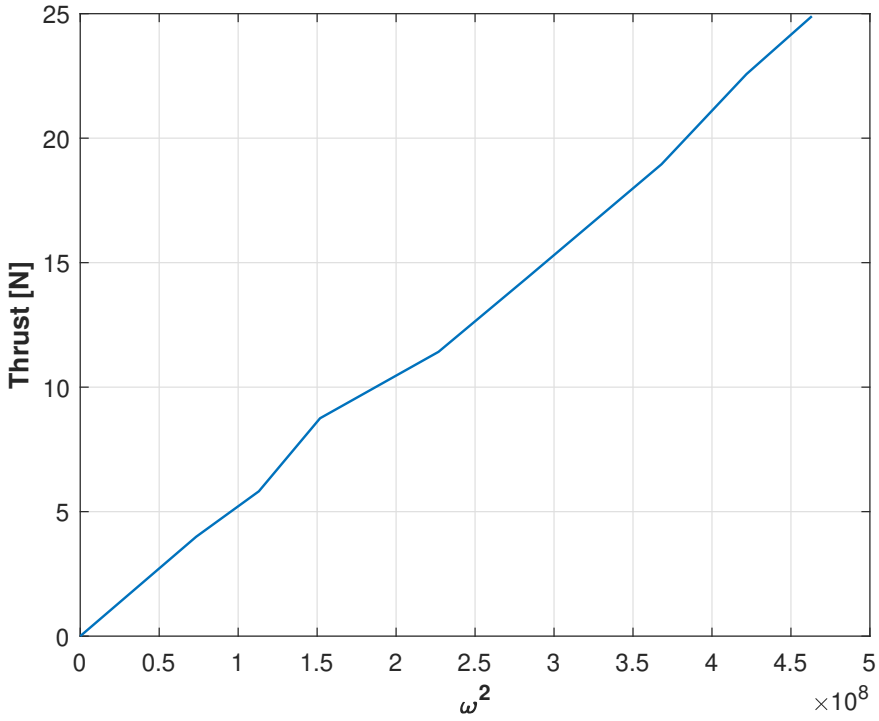

Figure 2.5 : Motor thrust vs RPM relationship.

The thrust and torque coefficients could be extracted from the motor and propeller test data. The motor used in this work is "BH SE 2807-1300KV" with a 7-inch propeller. According to the manufacturer's data tables, the relationship between the square of motor angular speed and thrust can be shown in Figure 2.5

While the relationship between motor angular speed and torque can be shown in Figure 2.6

Based on the given data, the motor model parameters can be illustrated in the table below 2.2

Table 2.2 : Motor parameters.

Parameter	Value	Description
l	0.1475 m	Distance between the rotors and CG
k_t	5.289e-8 N/RPM^2	Motor thrust coefficient
d	9.413e-11 $N.m/RPM^2$	Motor torque coefficient

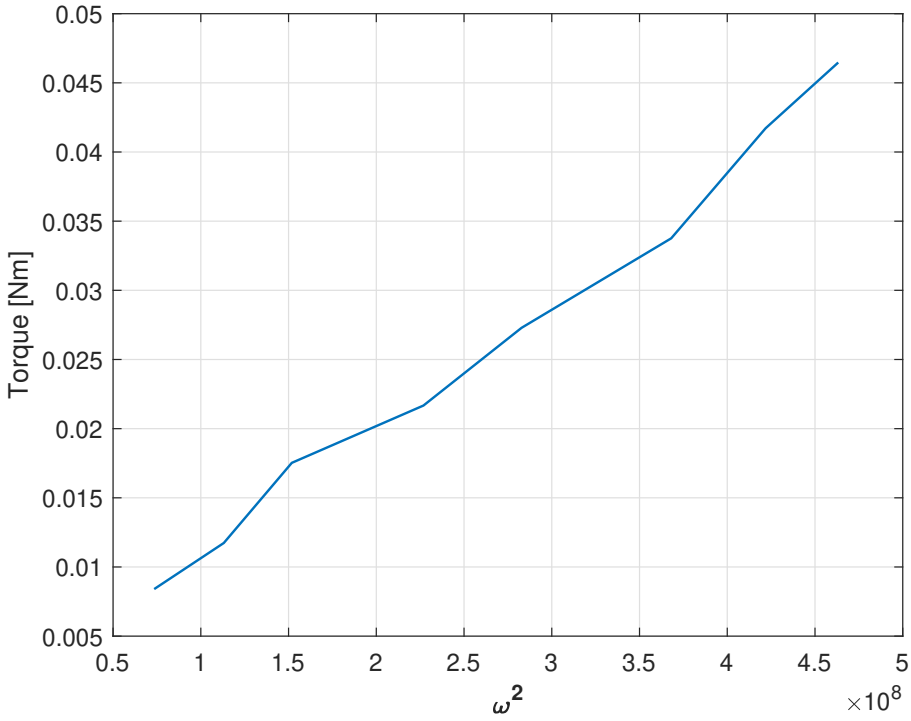

Figure 2.6 : Motor torque vs RPM relationship.

2.2.1 Actuator health and fault injection model

To account for actuator degradation and health monitoring, a motor health parameter W_i is introduced for each motor. This value ranges between $[0,1]$ where $W_i = 1$ represents full health (no degradation) and $W_i < 1$ indicates a partial loss of effectiveness (LOE). The thrust and moment generated by each motor are then modified by its health factor as follows:

$$T_i = W_i \cdot k_t \cdot \omega_i^2 \tag{2.23}$$

$$\tau_i = W_i \cdot d \cdot \omega_i^2 \tag{2.24}$$

To simulate faults and test the observer's robustness, I inject synthetic faults into the actuator system using one of the following models:

1. Step Loss of Effectiveness:

$$W_i(t) = \begin{cases} 1 & t < t_f \\ \alpha & t \geq t_f \end{cases} \tag{2.25}$$

   t_f is the fault occurrence time and $\alpha < 1$ is the degradation level.

2. Time-Varying Degradation:

$$W_i(t) = 1 - \beta(t - t_f), \quad t \geq t_f \tag{2.26}$$

   which simulates a gradual degradation over time. In both equations $W_i(t)$ is the actual motor health.

In summary, the actuator model is integrated with the dynamic equations to account for both normal operations and faulty conditions. This will help in the FDI system test and validation.

2.3 Aerodynamic and Wind Model

Environmental disturbances, such as wind and gusts, are crucial for this work, as they significantly impact the flight dynamics of quad-rotors, particularly for lightweight UAVs with limited payload and structural inertia. In addition, it will be used to verify and validate the FDI system under external disturbances.

In this study, a simplified wind model is used that incorporates both steady-state (constant) wind and short-duration gust components. The total wind force is applied directly in the inertial frame and is transformed into the body frame through the inverse of the rotation matrix R_{IB} for use in the dynamic equations.

The wind model can be expressed as:

$$F_{wind} = F_{steady} + F_{gust} \tag{2.27}$$

- F_{steady} is the constant component applied in a fixed direction, typically horizontal.
- F_{gust} is a transient function applied for a short duration to simulate a wind gust.

The total wind velocity is calculated as follows.

$$V_{wind} = V_{steady} + V_{gust} \tag{2.28}$$

where V is a three-element vector. While the steady wind is generated by a constant input and direction with respect to the north, the gust velocity is generated as a decaying pulse:

$$Vx_{gust}(t) = A_x \exp(-\frac{t - t_0}{\tau_g}) \tag{2.29}$$

$$Vy_{gust}(t) = A_y \exp(-\frac{t - t_0}{\tau_g}) \tag{2.30}$$

$$Vz_{gust}(t) = 0 \tag{2.31}$$

Where: A_x, A_y are the amplitudes of gust in x and y directions, t_0 is the start time of the gust, and τ_g is the decay constant, Then, the total wind force is calculated as follows

$$F_{wind} = \frac{1}{2}\rho V^2 A C_D \tag{2.32}$$

Where: ρ is the air density at the altitude, A is the body area, C_D is the drag coefficient.

This formulation enables the simulation to incorporate short wind bursts without necessitating more complex turbulence models. It can reflect the type of disturbances encountered during real-world operations, such as flying past obstacles or buildings. The wind force vector is added as an external force in the translational dynamic equation.

3. CONTROL STRATEGY

The primary aim of the controller is to stabilize the vehicle, track commanded trajectories, and reject external disturbances . Due to quad-rotors' inherent nonlinear and coupled dynamics, designing an effective control strategy poses significant challenges.

In this work, a cascaded model-based controller is implemented. The controller philosophy is based on the dynamic inversion concept. It enables the system to compensate for the nonlinear coupling between state variables by inverting the dynamics of the model, thus allowing for more intuitive and direct control law design. In addition, the motor health complementary observer proposed in this work primarily relies on the dynamic inversion controller.

The controller's stability and robustness in this work are very crucial since they directly affect the fault detection and isolation system's performance. Without a stable controller, the system may collapse before error estimation and definition.

The controller architecture consists of two main cascaded loops: the outer loop and the inner loop, followed by the control allocation stage. The outer loop deals with the translational motion and generates desired accelerations. These accelerations are transformed into attitude references for the inner loop, which then produces moment commands to achieve the desired orientations. The final step involves distributing these moments and thrusts to the individual motors through control allocation.

The overall control schematic is shown in Figure 3.1.

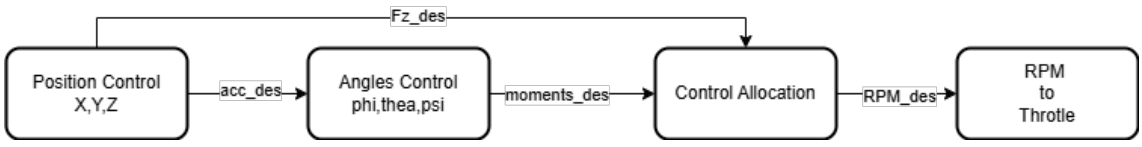

Figure 3.1 : Controller architecture.

3.1 Outer Loop Control

The outer control loops consist of three-state control loops. positions X, Y, and altitude Z control. The outer loop tracks reference trajectories in the inertial frame, controlling the desired velocity to achieve these trajectories. Based on the position and velocity errors, it computes the desired translational accelerations:

$$\dot{r}_d = K_p(r_d - r) \tag{3.1}$$

$$\ddot{r}_d = K_v(\dot{r}_d - \dot{r}) + K_i \int (\dot{r}_d - \dot{r})dt \tag{3.2}$$

Where:

- r is the 3D position vector in the inertial frame,
- r_d and $\dot{r}_d$ are the desired trajectory and velocity in the inertial frame.
- K_p and K_v are the proportional gains of position and velocity.
- K_i is an integrator term as compensation for aerodynamic drag and model uncertainty.

The desired acceleration is converted into a desired thrust vector, which in turn defines the required pitch and roll angles. Assuming the thrust acts along the body z-axis:

$$\mathbf{T}_d = m(\ddot{\mathbf{r}}_d + \mathbf{g}) \tag{3.3}$$

From the thrust vector, the desired roll and pitch angles are extracted using inverse trigonometric functions, while the yaw command is typically taken from a guidance law or kept constant.

3.2 Inner Loop Control

The inner loop uses the desired attitude to compute the angular rate references and apply dynamic inversion. The nonlinear attitude dynamics (using body rates) are given by:

$$\tau_d = \mathbf{I}\dot{\omega}_d \tag{3.4}$$

where I is the inertia matrix and ω is the angular velocity vector. The desired angular acceleration vector is being computed as:

$$\omega_d = K_p\,(e_d - e) \tag{3.5}$$

$$\dot{\omega}_d = K_d(\omega_d - \omega) + K_i \int (\omega_d - \omega) \tag{3.6}$$

Where:

- e is the 3D Euler angle vector,
- ω_d and $\dot{\omega}_d$ are the desired angular velocity and acceleration,
- K_p and K_d are the proportional and derivative gains of angle and angular velocity.
- K_i is an integrator term as compensation for aerodynamic drag and model uncertainty.

3.3 Control Allocation

The desired thrust and torques are translated into motor speeds through a control allocation matrix. Based on the relationship between the motor's angular speed, thrust, and torque mentioned in the past chapter, the thrust and torque coefficients can be calculated using the motor and propeller test data. After calculating the coefficient, the actuator mapping can be as follows:

$$\begin{bmatrix} \omega_1^2 \\ \omega_2^2 \\ \omega_3^2 \\ \omega_4^2 \end{bmatrix} = \mathbf{A}^{-1} \begin{bmatrix} T_d \\ \tau_{\phi d} \\ \tau_{\theta d} \\ \tau_{\psi d} \end{bmatrix} \tag{3.7}$$

Where A is the control effectiveness matrix, which includes the motor and propeller dynamics mentioned in 2.22.

The desired motor angular rates can be calculated by pseudo-inverting the A matrix. Later, the motor health factors can be added to the allocation to tolerate the motor fault. [12]

$$\mathbf{A}^{-1} = (A^T * A)^{-1} * A^T \tag{3.8}$$

3.4 RPM to Throttle Command

Once the desired motor speeds (angular velocities) are calculated through the control allocation matrix, it is necessary to convert these values into appropriate throttle commands that control the motor's behavior. Given that the motor RPM is directly linked to the throttle input, this conversion process plays a critical role in ensuring that the system remains responsive and efficient.

To simplify this process, a second-order relationship between throttle and motor RPM was derived from motor test data. This empirical relationship enables the mapping of the desired RPM to the corresponding throttle command without the need for a lookup table, thereby maintaining software efficiency. A first-order model was selected to approximate the motor's response, which provides a good balance between computational complexity and accuracy.

The RPM command is mapped to the throttle command using the following empirical first-order relationship:

$$throttle_{cmd} = a_1 \cdot \text{RPM} + a_0 \tag{3.9}$$

Where a_0 and a_1 are constants derived from motor test data, and RPM represents the desired motor speed. This relationship ensures that the throttle command corresponds

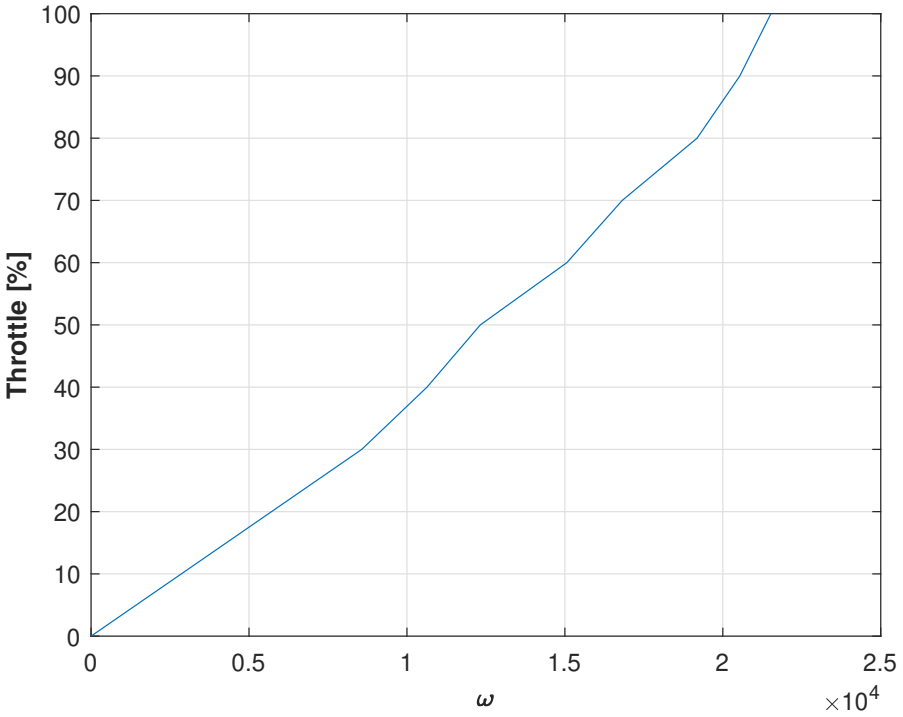

Figure 3.2 : Motor thrust vs RPM relationship.

to the motor's RPM in a computationally efficient manner, thereby avoiding the need for large lookup tables in the autopilot software.

Table 3.1 : RPM to throttle coefficients.

Coefficient	Value
a_0	-5.5
a_1	0.004571

To further enhance the realism and simulate motor dynamics more accurately, the throttle command is then rounded to the nearest integer using the ceiling function. This ensures that the throttle input is always an integer value, which reflects the discrete nature of motor control in real-world systems.

By applying this approach, the system remains efficient while still capturing the necessary motor dynamics and control behavior. The use of the second-order relationship instead of a lookup table reduces computational load, which is essential for real-time operation. Additionally, the ceiling function helps simulate the discrete

nature of motor control, improving the accuracy of the simulation and the overall system performance.

3.5 Controller Gain Selection and Tuning

The controller gain selection in this work is based on shaping the closed-loop response to follow the behavior of a second-order system with desired performance metrics. This methodology ensures that both the position and attitude controllers achieve the required responsiveness and stability.

For each controlled state, the desired closed-loop dynamics are characterized by a second-order system:

$$\ddot{x} + 2\zeta\omega_n\dot{x} + \omega_n^2 x = \omega_n^2 x_d \tag{3.10}$$

where:

- x_d is the desired value,
- ω_n is the natural frequency,
- $\zeta$is the damping ratio.

By comparing this desired dynamic with the actual control law, the proportional and derivative gains can be chosen as:

$$K_p = \omega_n^2 \tag{3.11}$$

$$K_d = 2\zeta\omega_n \tag{3.12}$$

This approach is applied to the translational outer and rotational inner loops. Typical values used for tuning were selected to achieve a critically damped or slightly under-damped response ($\zeta = 0.7\ -1$) with a natural frequency adjusted based on the dynamic range of the respective control loop.

The gain selection was validated through iterative simulations, confirming that the system exhibits acceptable transient and steady-state behavior in the presence of noise, model uncertainties, and actuator effectiveness degradation.

4. FAULT DETECTION AND ISOLATION SYSTEM

Quadrotor UAVs are inherently nonlinear, underactuated, and open-loop unstable, making their flight dynamics highly sensitive to actuator faults. Failures such as loss of effectiveness (LOE), intermittent behavior, or complete motor failure can cause significant degradation in flight stability and even lead to catastrophic mission failure. The reliability of these systems is critically dependent on the performance of their actuators, particularly the brushless DC motors that generate lift and enable control.

To address this challenge, robust Fault Detection and Isolation (FDI) systems are essential. These systems aim to detect abnormal behavior in actuators at an early stage, identify the affected component, and enable the integration of fault-tolerant control measures to preserve system integrity. Unlike traditional methods that rely on redundant sensors or actuator feedback—approaches that may increase system weight, cost, and complexity—this thesis proposes a purely model-based FDI system.

The proposed approach integrates two complementary mechanisms: a nonlinear Thau observer for tracking system states and estimating output residuals, and a dynamic inversion-based residual observer that exploits the mismatch between commanded and estimated actuator behavior. Together, these mechanisms enhance the system's capability to detect actuator faults, isolate their location, and estimate their severity. Overall system architecture illustrated in Figure 4.1.

The FDI architecture is designed to operate without requiring direct actuator feedback or redundant sensors, which makes it suitable for lightweight UAV platforms. It is also structured to be robust against modeling uncertainties, sensor noise, and environmental disturbances. By evaluating the discrepancy between measured and estimated outputs (residuals), the system can identify both sudden and gradual faults with high sensitivity.

This chapter presents the fault scenarios and underlying assumptions, followed by the design, mathematical formulation, and implementation of both FDI components. The

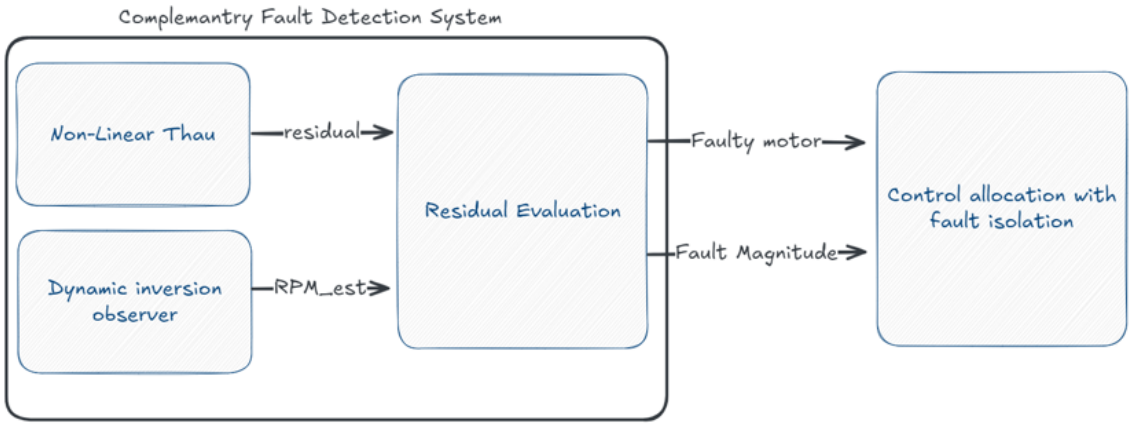

Figure 4.1 : FDI system architecture

residual evaluation strategy and fault isolation methodology are discussed in detail, the fault magnitude estimation methodology, and finally, the fault-tolerant control allocation approach is described.

4.1 Fault Scenarios and Model Assumptions

4.1.1 Fault scenarios

The faults targeted in this work are limited to **Loss of Effectiveness (LOE)** faults in the motors. These faults are represented as a reduction in the actuator's ability to generate the expected thrust or torque. The following two forms of LOE are simulated and evaluated:

- **Sudden LOE Faults**: A motor experiences an instantaneous drop in effectiveness at a specified time. This models faults such as rapid motor degradation or partial mechanical/electrical failure.
- **Gradual/Time-Varying LOE Faults**: A motor's effectiveness deteriorates progressively over time. This type of fault models issues like gradual wear, increased friction, or temperature-induced performance degradation.

Each LOE fault is modeled using a time-varying effectiveness factor $W_i(t) \in [0,1]$ for motor i, where $W_i(t) = 1$ corresponds to a fully healthy motor and $W_i(t) < 1$ reflects a

degradation in performance. A value of $W_i(t) = 0$ indicates total failure.

$$F_{i,\text{actual}} = W_i(t) \cdot F_{i,\text{cmd}} \tag{4.1}$$

This multiplicative fault model is commonly used in literature due to its simplicity and compatibility with control allocation strategies.

4.1.2 Modeling Assumptions

The FDI system design is based on a set of practical and simplifying assumptions that are typical for embedded UAV systems:

- **No Direct Motor Feedback**: The health of the motors is not measured directly through sensors such as RPM encoders or current measurements. All fault information is inferred through estimation-based residual analysis.
- **Model Uncertainties**: The parameters of the system (e.g., mass, inertia) deviate slightly from their nominal values due to environmental factors or unmodeled dynamics. However, these deviations are assumed to be within known bounds.
- **Sensor Noise**: Measurements are affected by additive noise, which is assumed to be zero-mean and bounded. The observer design incorporates robustness to reject such noise without introducing false alarms.
- **Actuator Faults Only**: This work does not consider faults in the sensor suite (e.g., IMU or GPS) or software-related faults. The FDI system is solely focused on motor health estimation.

By establishing these assumptions, the observer structure and residual evaluation strategies can be tailored to focus on actuator performance and minimize the influence of unrelated disturbances or unmodeled sensor issues. These assumptions also align with the implementation context of lightweight UAVs, where minimizing sensor complexity is often a design goal.

4.2 Non-Linear Thau Observer

In this work, a nonlinear Thau observer is adopted for state reconstruction and fault detection. Linear Thau observers and most linear techniques rely on linearized dynamics around a nominal operating point. In contrast, the nonlinear formulation is more suitable for quad-rotor systems due to their inherently nonlinear, coupled, and time-varying nature. Using a nonlinear observer ensures accurate state estimation across the entire flight envelope, avoiding the limitations and inaccuracies introduced by linearization. The Thau observer is used to estimate the full state vector of the system using available sensor measurements and known control inputs. It is designed based on the nominal nonlinear model of the quad-rotor. The basic observer structure is defined as:

$$\dot{\hat{x}}(t) = f(\hat{x}(t), u(t)) + K \cdot r(t) \tag{4.2}$$

where:

- $\hat{x}(t)$ is the estimated state vector,
- $f(\hat{x}(t), u(t))$ represents the nonlinear dynamics of the system,
- K is the observer gain matrix,
- $r(t)$: residual vector, $r(t) = y(t) - \hat{y}(t)$

The estimated output $\hat{y}(t)$ is computed from the estimated states as:

$$\hat{y}(t) = C \cdot \hat{x}(t) \tag{4.3}$$

where C is the output matrix that maps the state variables to the measured outputs. The system in the state space form can be described as follows: The estimated states

$$x(t) = \begin{bmatrix} x & y & z & v_x & v_y & v_z & \phi & \theta & \psi & p \\ q & r & & & & & & & & \end{bmatrix}^T \tag{4.4}$$

$$\dot{x}(t) = \begin{bmatrix} \dot{x} & \dot{y} & \dot{z} & \dot{v}_x & \dot{v}_y & \dot{v}_z & \dot{\phi} & \dot{\theta} & \dot{\psi} & \dot{p} \\ \dot{q} & \dot{r} & & & & & & & & \end{bmatrix}^T \tag{4.5}$$

while the measurement vector is as follows:

$$y(t) = \begin{bmatrix} x & y & z & \phi & \theta & \psi \end{bmatrix}^T \tag{4.6}$$

The control input vector includes the total thrust and the three control torques generated by the motors:

$$u(t) = \begin{bmatrix} T & \tau_\phi & \tau_\theta & \tau_\psi \end{bmatrix}^T \tag{4.7}$$

The nonlinear function $f(\hat{x}(t), u(t))$ represents the Newton-Euler equations governing the translational and rotational dynamics of the quad-rotor.

4.2.1 Translational dynamics

The translational dynamics used in the Thau observer starts from calculating the linear accelerations as follows:

$$\begin{aligned} \dot{v}_x &= \frac{1}{m}\left[(\cos\phi \sin\theta \cos\psi + \sin\phi \sin\psi)T\right] \\ \dot{v}_y &= \frac{1}{m}\left[(\cos\phi \sin\theta \sin\psi - \sin\phi \cos\psi)T\right] \\ \dot{v}_z &= \frac{1}{m}\left[-(\cos\phi \cos\theta)T\right] - g \end{aligned} \tag{4.8}$$

where $\dot{v}$ are the accelerations in the inertial frame. Once the accelerations are calculated, the velocity and position according to the inertial frame could be calculated by applying Euler integration.

$$v = \int \dot{v} dt \tag{4.9}$$

$$x = \int v dt \tag{4.10}$$

where v and x are three element vectors.

4.2.2 Rotational dynamics

The rotational dynamics used in the observer starts from calculating the angular accelerations as follows :

$$\begin{aligned}
\dot{p} &= \frac{1}{I_{xx}}\left[\tau_\phi - (I_{zz} - I_{yy})qr\right] \\
\dot{q} &= \frac{1}{I_{yy}}\left[\tau_\theta - (I_{xx} - I_{zz})pr\right] \\
\dot{r} &= \frac{1}{I_{zz}}\left[\tau_\psi - (I_{yy} - I_{xx})pq\right]
\end{aligned} \tag{4.11}$$

Euler angle rates:

$$\begin{aligned}
\dot{\phi} &= p + q\sin\phi\tan\theta + r\cos\phi\tan\theta \\
\dot{\theta} &= q\cos\phi - r\sin\phi \\
\dot{\psi} &= q\sin\phi/\cos\theta + r\cos\phi/\cos\theta
\end{aligned} \tag{4.12}$$

After angular velocity and acceleration calculation, Euler angles and body angular rates can also be achieved by Euler integration.

$$\begin{bmatrix} p \\ q \\ r \end{bmatrix} = \int \begin{bmatrix} \dot{p} \\ \dot{q} \\ \dot{r} \end{bmatrix} dt \tag{4.13}$$

$$\begin{bmatrix} \phi \\ \theta \\ \psi \end{bmatrix} = \int \begin{bmatrix} \dot{\phi} \\ \dot{\theta} \\ \dot{\psi} \end{bmatrix} dt \tag{4.14}$$

4.2.3 Residual generation

After the estimated states are computed by the Thau observer, the residuals are obtained by taking the difference between the actual measurements and the corresponding estimated outputs, as shown in equation 4.15.

$$r(t) = y(t) - \hat{y}(t) \tag{4.15}$$

Specifically:

$$\begin{aligned}
r_1(t) &= x(t) - \hat{x}(t) \\
r_2(t) &= y(t) - \hat{y}(t) \\
r_3(t) &= z(t) - \hat{z}(t) \\
r_4(t) &= \phi(t) - \hat{\phi}(t) \\
r_5(t) &= \theta(t) - \hat{\theta}(t) \\
r_6(t) &= \psi(t) - \hat{\psi}(t)
\end{aligned} \tag{4.16}$$

Although the observer generates six residual signals—three for position and three for attitude— in this work, only the attitude residuals (r_4, r_5, r_6) are utilized for fault detection. This is because actuator (motor) faults have a much more immediate effect on the vehicle's attitude than on its position. By focusing on attitude residuals, the fault detection system can identify and estimate actuator faults more rapidly, thereby reducing the detection latency and improving system responsiveness.

4.2.4 Observer gain matrix

K is tuned such that the observer remains stable and ensures rapid convergence of residuals without amplifying measurement noise. Typically, K is diagonal and set based on simulation or via optimization.

4.3 Dynamic Inversion Complementary Observer

While the nonlinear Thau observer can estimate the full state vector and track system behavior using the system model, it can not directly identify fault type or magnitude. This work introduces a complementary observer based on dynamic inversion to enhance fault detectability, especially in the presence of gradual or partial actuator faults.

The proposed dynamic inversion-based observer estimates the expected actuator response by back-calculating the forces and moments from the measured system accelerations. This information is then used to reconstruct and compare the estimated motor speeds with the controller's desired motor speeds. The discrepancy between the estimated and desired motor speeds forms a secondary residual signal, enabling a more robust and interpretable fault detection strategy.

This dual-residual approach, combining state estimation errors with actuator-level residuals, enables:

- Improved fault isolation
- Redundant fault detection enhances reliability under noisy or model-uncertain conditions.

- Ability to tolerate the LOF faults and support controller stability in the presence of a fault.

4.3.1 Mathematical Formulation

The process can be summarized in three main steps:

Step 1: Estimating Force and Moment from Acceleration

The actual force and moment applied to the body are estimated as follows, assuming thrust is the only significant force in the body z direction and neglecting external disturbances such as aerodynamic drag and wind forces :

$$F_{z,\text{est}} = m\left(a_{z,\text{meas}} - g\right) \tag{4.17}$$

$$\tau_{\text{est}} = I \cdot \dot{\omega}_{\text{est}} \tag{4.18}$$

Where:

- m is the mass of the quadrotor,
- $a_{z,meas}$ is the body-frame translational acceleration measured by IMU in z direction,
- g is the gravitational acceleration,
- I is the diagonal inertia matrix,
- $\dot{\omega}_{est}$ is the derivative of the angular velocity measured by the gyro.

Step 2: Mapping Force and Moment to Motor Speeds The estimated collective thrust and moments are grouped as:

$$u_{est} = \begin{bmatrix} F_{z_{est}} & \tau_{\phi est} & \tau_{\theta est} & \tau_{\psi est} \end{bmatrix}^T \tag{4.19}$$

The squared motor speeds can be estimated using the inverse of the control effectiveness matrix A:

$$\omega^2 = A^{-1} u_{est} \tag{4.20}$$

$$\omega_{est,i} = \sqrt{\omega^2} \tag{4.21}$$

where A models the relationship between motor speeds and generated forces/moments, as defined in Chapter 3.

Step 3: Motor Health Generation

The motor health is being generated by comparing the estimated motor angular speed with the desired angular speed.

$$W_i = \frac{\omega_{est,i}}{\omega_{exp,i}} \tag{4.22}$$

The resulting motor health indicator W_i is ideally within $[0, 1]$, but practical factors such as measurement noise and model uncertainties may extend this range slightly above 1 (e.g., up to 1.2).

4.3.2 Practical implementation

There are some practical considerations regarding the estimation of the motor's angular speed.

1. The angular acceleration is estimated using discrete differentiation of the measured angular rates, which are measured by a gyro. To avoid numerical instability and spurious spikes, angular velocity signals are first passed through a low-pass filter before differentiation. This helps ensure stable estimation of $\dot{\omega}_B$.

2. The commanded motor speeds issued by the controller do not perfectly reflect the expected angular speeds due to internal motor dynamics. To account for this, a first-order model of the motor is implemented:

$$\omega_{\text{exp}} = \frac{1}{\tau_m s + 1} \cdot \omega_{\text{cmd}} \tag{4.23}$$

Where τ_m is the motor time constant. This filtered signal is used as the baseline expected RPM.

The motor health, combined with the Thau observer outputs, forms a robust model-based FDI system capable of detecting and isolating actuator faults in real-time

using only onboard measurements and known dynamics. The next section presents the residual evaluation logic, thresholding methodology, and how both observer outputs are fused to make a final fault decision.

4.4 Residuals Evaluation

The core function of any Fault Detection and Isolation (FDI) system is to interpret residual signals in a reliable manner and distinguish between nominal behavior and faulty conditions. In this work, a structured residual evaluation strategy is proposed. It includes fault decision logic, an adaptive thresholding mechanism to enhance robustness, and a magnitude estimation approach that provides further insight into fault severity.

4.4.1 Fault detection and isolation mechanism

In the proposed FDI system, two residual streams are generated, and a combined residual evaluation strategy has been applied. As a total, there are four residual signals used in the fault detection and isolation process. To avoid false positives and increase reliability, both residuals are evaluated independently. A fault is declared only when residuals from both observers exceed their respective thresholds consistently over a time window. The fault detection and isolation strategy is illustrated in the table below 4.1:

Table 4.1 : Fault detection and isolation mechanism.

residual	Motor 1	Motor 2	Motor 3	Motor 4
r_ϕ	$-$	$+$	$+$	$-$
r_θ	$-$	$-$	$+$	$+$
r_ψ	$+$	$-$	$+$	$-$
W	$< \delta_w$	$< \delta_w$	$< \delta_w$	$< \delta_w$

The proposed decision logic ensures high confidence in fault isolation without needing additional sensors.

4.4.2 Adaptive threshold

Due to the changing measurement noise and external disturbances, fixed thresholds may either miss faults or generate false alarms. To address this, we implement

an adaptive thresholding mechanism based on the statistical properties of the measurement during nominal operation, and on the ground before taking off. The adaptive threshold st The adaptive threshold for each residual channel is computed as:

$$\delta_i(t) = k_\sigma \cdot \sigma_i(t) \tag{4.24}$$

Where:

- $\sigma_i(t)$ is the standard deviation of measurements over a sliding time window.
- k_σ is a tuning constant that scales sensitivity.

These values are updated online and used to distinguish between acceptable deviations due to noise and actual fault indicators.

4.5 Fault Magnitude Estimation

In addition to fault detection, estimating the severity of an actuator fault is critical for enabling fault-tolerant control and reconfiguration strategies. In this work, the fault magnitude is interpreted as the Loss of Effectiveness (LOE) of each motor and is computed using actuator residuals derived from the dynamic inversion observer.

The motor health index $W_i(t)$—defined as the ratio between the estimated motor angular velocity and its expected value—is used to infer the degree of effectiveness. The fault magnitude $\gamma_i(t)$ for motor i is then estimated as:

$$\gamma(t) = \begin{cases} 1 - W_i, & t > (t_{fault} + t_w) \\ 1 - \mu(W_i), & \frac{\delta\mu(W_i)}{dt} < th_\gamma \end{cases} \tag{4.25}$$

where:

- $\gamma(t)$ is the estimated fault magnitude, representing the relative loss of effectiveness,
- W_i is the health indicator of motor i as defined in Section 4.3,
- $\mu(\cdot)$ represents a smoothing operator - windowed average - to reduce transient noise effects,

- t_w is a time window to estimate the slow fault magnitude,
- th_γ is a small value threshold.

This estimate is only considered valid and reported when the health residual exceeds its adaptive threshold δ_w, ensuring robustness against sensor noise and false alarms during nominal operation.

To avoid misinterpretation during transient disturbances or rapid attitude changes, the estimation process of fault magnitude is designed in two stages:

Fast Estimation Phase: Triggered immediately after fault detection, this stage provides a rapid one-time approximation of fault magnitude to support timely stabilization. It uses a short sliding window to produce a fast-reacting.

Slow Estimation Phase: After the fast response settles, a longer sliding window is applied to extract the steady-state behavior of the fault. The resulting estimate is being used for long-term control adaptation and reporting. This two-stage approach ensures both responsiveness and reliability by filtering out transient inaccuracies.

In practice, the motor health $W_i(t)$ is monitored continuously, and a transition from the fast to slow estimator is handled internally using a logic flag or timer mechanism once the residual stabilizes. This dual-stage magnitude estimation allows the system to respond quickly while avoiding misclassifying transient dynamics as persistent degradation. The control allocation module can then use the final $\gamma_i(t)$ estimate to re-weight motor contributions or activate fault-tolerant strategies.

4.6 Tolerated Control Allocation

After a fault is detected and its magnitude is estimated, the control allocation system is adopted to preserve stability and ensure that the quadrotor can continue to execute its mission. This work implements a fault-tolerant control allocation method by incorporating a dynamic weight matrix that reflects the effectiveness of each motor.The

control effectiveness is adjusted through a health matrix $W \in \mathbb{R}^{4\times4}$ defined as:

$$W = \begin{bmatrix} (1-\gamma_1)^2 & 0 & 0 & 0 \\ 0 & (1-\gamma_2)^2 & 0 & 0 \\ 0 & 0 & (1-\gamma_3)^2 & 0 \\ 0 & 0 & 0 & (1-\gamma_4)^2 \end{bmatrix} \tag{4.26}$$

This matrix modifies the control allocation as follows:

$$\omega^2 = W^{-1} \cdot A^{-1} \cdot u_d \tag{4.27}$$

Where:

- $u_d = [T_d, \tau_{\phi d}, \tau_{\theta d}, \tau_{\psi d}]^T$ is the desired control input vector,
- A is the nominal control effectiveness matrix (relating motor speeds to generated forces/moments),
- ω^2 is the resulting squared motor speeds after fault-tolerant allocation.

This implementation allows seamless integration with the existing control system. When a motor fault is detected, its control contribution is proportionally reduced according to the estimated fault magnitude. The health matrix dynamically adjusts each diagonal entry to represent the remaining effectiveness of each motor. If no fault is detected or fault isolation is deactivated, the matrix defaults to the identity matrix, preserving nominal allocation. This structure ensures system stability by reweighting motor effectiveness during partial LOE faults.

4.7 Summary

This chapter presented the complete design of the fault detection and isolation system used in this work. Beginning with the fault scenarios and system assumptions, we introduced two complementary observer structures—the nonlinear Thau observer and the dynamic inversion-based observer. Each was described in detail, including their formulation, implementation, and roles in detecting and isolating actuator faults. A robust residual evaluation strategy was then developed, integrating adaptive thresholds and fault magnitude estimation. Finally, a fault-tolerant control allocation mechanism

was proposed to ensure the system remains controllable even under degraded motor conditions.

In the next chapter, we turn to simulation and validation. We demonstrate the behavior of the full system under various fault scenarios and environmental disturbances, validating the effectiveness of the proposed FDI framework in realistic conditions.

5. SIMULATION AND RESULTS

In this chapter, the simulation environment used to test and validate the proposed Fault Detection and Isolation (FDI) system for a quadrotor Unmanned Aerial Vehicle (UAV) is presented.

5.1 Simulation Environment

The MATLAB-Simulink environment was developed, containing both the nonlinear dynamic model of the quad-rotor, controller, and FDI system. The non-linear Thau observer is implemented as an S-function using *c* programming language to ensure a real-time and realistic discrete response. The simulations were designed to closely simulate realistic flight conditions by integrating external disturbances, sensor noise, and actuator dynamics.

A high-fidelity representation of the physical parameters was ensured, reflecting the behavior of the quadrotor platform mentioned in chapter 2. The simulation was conducted in MATLAB/Simulink using a fixed-step solver (ode3) with a step size of 1 ms (1000 Hz) to guarantee numerical integration stability and preserve signal integrity, especially during fault transitions.

5.1.1 Initial conditions

A flight mode manager is designed for the system, and the aircraft begins on the ground in the disarm mode, located at the origin of the inertial frame. It has zero linear and angular velocities and zero level attitude, and its roll, pitch, and yaw angles are set to zero degrees. These conditions replicate a typical take-off scenario where the vehicle is initially at rest on the ground.

At the beginning of the take-off mode, the nonlinear Thau observer is initialized with the current measurement values. The residual generation process is initiated on the ground in disarm mode and begins with take-off mode after initialization is complete.

Additionally, the adaptive threshold windows are calculated on the ground and provide the threshold values during the takeoff process.

5.2 Test Scenarios

Several simulation scenarios were designed to reflect various actuator fault conditions, allowing for a thorough assessment of the robustness and responsiveness of the proposed Fault Detection and Isolation (FDI) framework. These scenarios aim to validate the system's ability to detect, isolate, and estimate fault types under practical operating conditions. The scenarios also evaluate the system's resilience against external disturbances, modeling errors, and measurement noise.

The fault types selected for testing are based on common and critical actuator faults encountered in quad-rotor UAVs—specifically, loss of effectiveness (LOE) motor faults. These faults are introduced in two distinct forms:

1. **Sudden LOE Faults:** Simulate an abrupt and significant drop in the effectiveness of a motor. This type of fault is designed to emulate fast-developing mechanical or electrical failures, such as winding burns or connector disconnections. In these tests, the motor's effectiveness drops instantaneously at a predefined time (20 s).

2. **Gradual LOE Faults:** Represent a more complex degradation in actuator performance that appears over time. These scenarios model progressive conditions, such as increased friction, dust accumulation, or thermal wear. In simulation, the motor health factor gradually decreases over a 25-second time window.

Faults are injected individually into each motor to assess the system's ability to isolate the faulty actuator and estimate the severity of degradation. For each simulation run, only one motor is subjected to a fault, ensuring clarity of residual behavior and fault source attribution. To keep the simulation realistic, every test type was conducted in two conditions:

1. **Normal conditions** with low noise level and without any external disturbances.

2. **External disturbances** such as wind, gusts, and higher sensor noise.

Table 5.1 : Verification test conditions.

Test condition	Value
Wind	$3\ m/s$
Gust	$2\ m/s$ @ 10s
Noise	$\sigma = 2$ deg
Faulty model parameter	15% error factor in inertia

The noise level applied to the measurements can be shown in Figure 5.1 below.

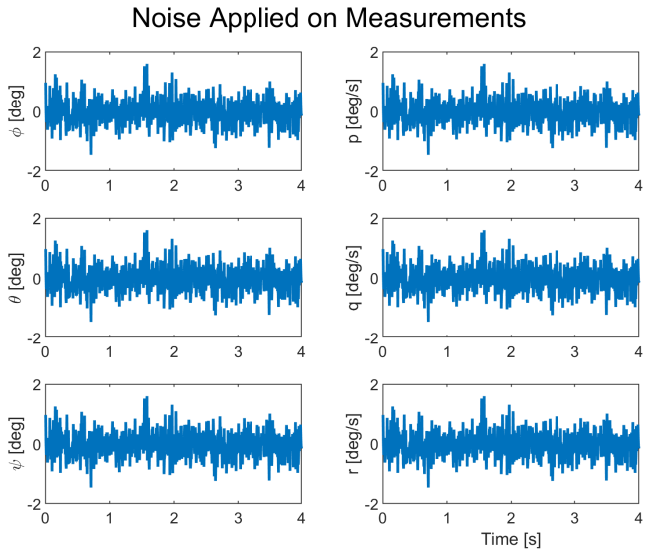

Figure 5.1 : Measurement noises.

The simulation spans 60 seconds per run in the sudden LoE tests and 120 seconds for the gradual LoE tests. The simulation runs allow sufficient time to observe the detection process, estimation, and control adaptation cycle.

Multiple fault scenarios were simulated under varied operating conditions. The test framework is designed to be both configurable and repeatable, allowing consistent performance benchmarking across all simulations.

Scenario 1: Nominal Operation In this case, the system operates without any actuator fault. The purpose of the test is to verify system stability, controller performance, and observer residual behavior in ideal conditions. All residuals and health indicators should remain within nominal ranges.

Scenario 2: Sudden LOE Fault A sudden loss-of-effectiveness (LOE) fault is introduced in one motor during mid-flight at the 20th second. The thrust contribution of this motor is instantaneously reduced to 80% of its nominal value.

Scenario 3: Gradual LOE Fault In this case, the motor effectiveness decays slowly over time. The fault starts at the 20th second with 80% efficiency and linearly drops to 60% over several seconds. In every test, the aircraft was commanded to complete its mission until it returned to the initial point. The mission consists of a square trajectory, beginning from the aircraft's initial point and returning to it.

This comprehensive set of test cases serves as a foundation for analyzing the FDI system's performance in the following sections, where metrics such as detection time, residual behavior, and estimation accuracy will be presented and discussed.

5.3 Results and Analysis

This section presents the simulation results obtained from the test scenarios mentioned in the last section. The evaluation focuses on the performance of fault detection and isolation. The key performance indicators include detection time, false alarm rate, and control stability after the fault.

5.3.1 Performance Metrics

The evaluation of the FDI system is based on the following criteria:

Table 5.2 : Performance metrics.

Criteria	Explanation
Detection Time	Time elapsed from the fault occurrence to detection.
False Alarm Rate	Number of Incorrect Fault Indications.
Fault Magnitude Estimation	Accuracy of the fault magnitude indicator γ.

These metrics offer a comprehensive view of both the detection quality and the system's ability to maintain stability.

5.3.2 Nominal conditions

Under nominal conditions, all observer residuals remained within their thresholds, confirming the absence of false alarms. The tracking error was minimal. The motor health indicators correctly stayed near unity, indicating no degradation.

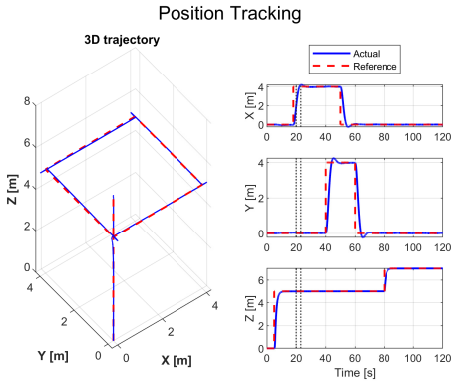

((a)) Position Tracking

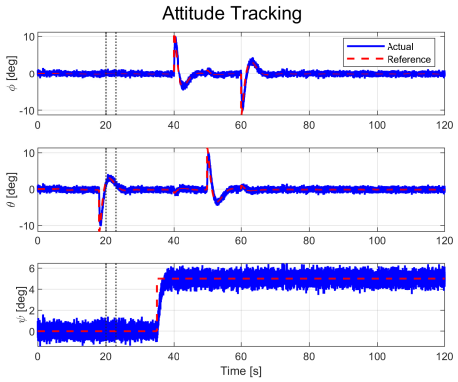

((b)) Attitude Tracking

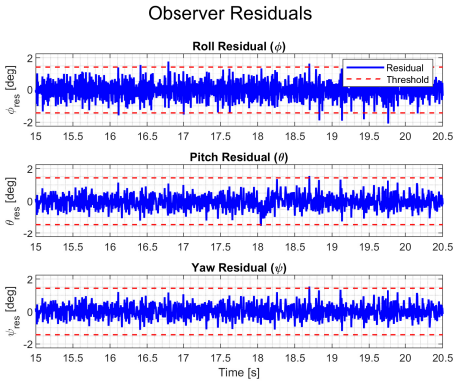

((c)) Residuals

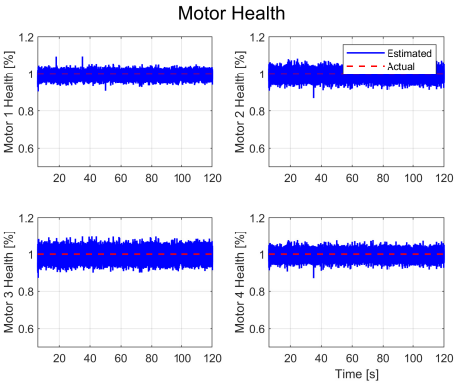

((d)) Motor Health

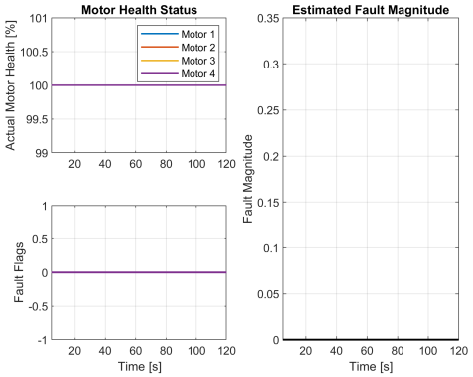

((e)) Motor Fault Flags

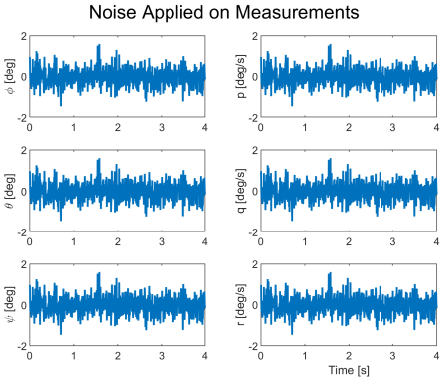

((f)) Measurements noise

Figure 5.2 : Nominal condition test scenario.

5.3.3 Sudden loss of effectiveness (LOE)

In the sudden LOE scenario, the system successfully detected the fault within 0.15–0.25 seconds. The attitude residuals (especially roll and pitch) exhibited a sharp increase immediately after the fault. The dynamic inversion-based observer produced consistent drops in motor health estimates, matching the injected loss. Fault magnitude estimation settled to a steady-state value with less than 5% error, and the reconfigured controller maintained trajectory tracking and mission completion without instability.

The first figure shows the controller performance during and after the sudden LoE fault for the first motor.

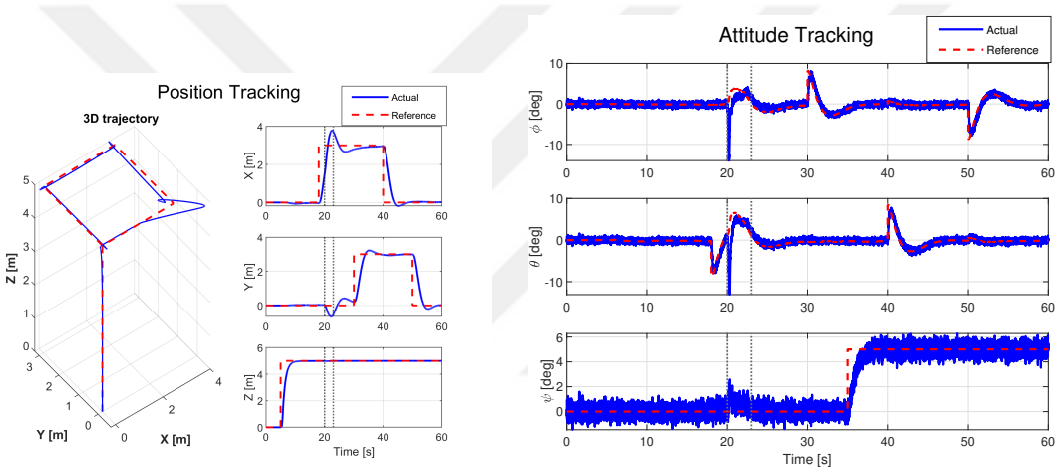

((a)) Position Tracking ((b)) Attitude Tracking

Figure 5.3 : Motor 1 sudden LoE controller performance.

Figure 5.4 shows the controller tracking during and after the sudden LoE fault for the first motor, while Figure 5.4 shows the FDI system performance.

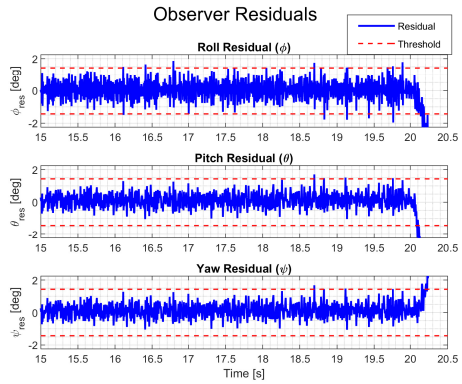

((a)) Residuals

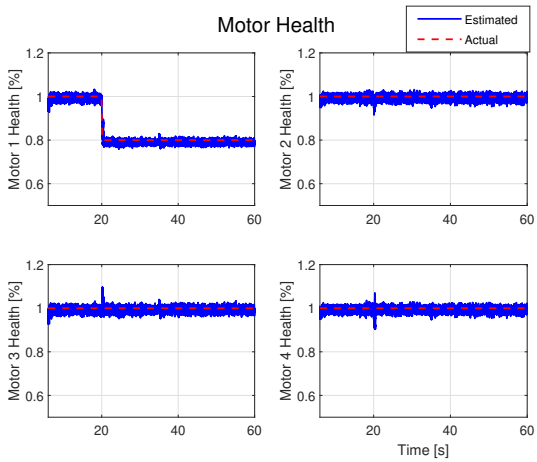

((b)) Motor Health

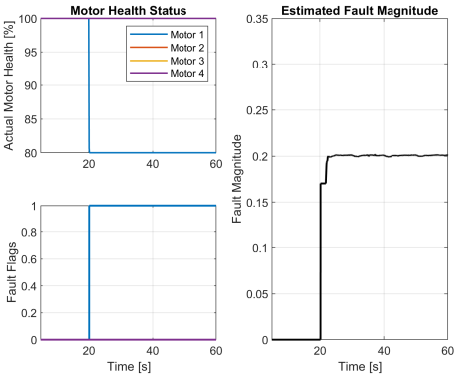

((c)) Motor fault flags and magnitude

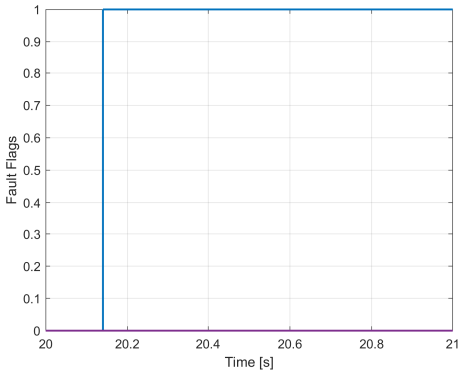

((d)) Fault flags

Figure 5.4 : Motor 1 sudden LoE FDI system performance.

The second set of figures shows the response of the second motor during and after sudden LoF faults. It can be noticed that the fault flag for Motor 2 is raised in less than 0.2 seconds, and the estimated fault magnitude aligns well with the actual loss.

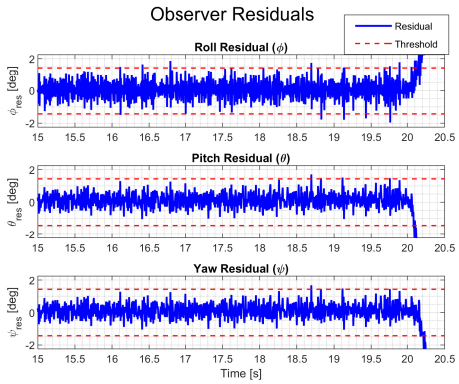

((a)) Residuals

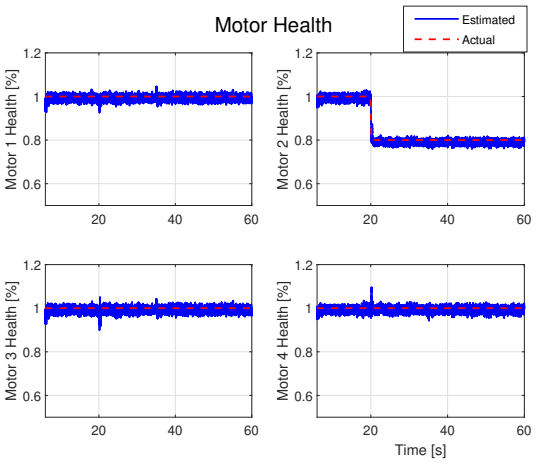

((b)) Motor Health

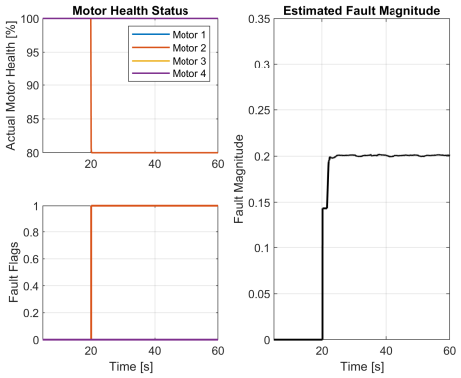

((c)) Motor fault flags and magnitude

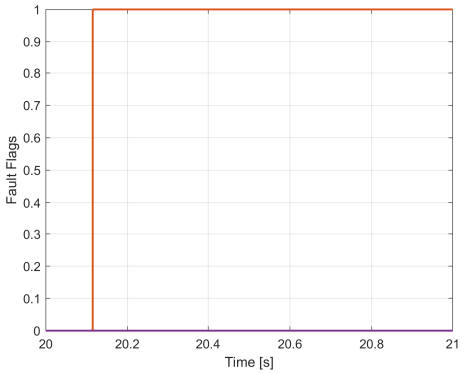

((d)) Fault flags

Figure 5.6 : Motor 2 sudden LoE FDI system performance.

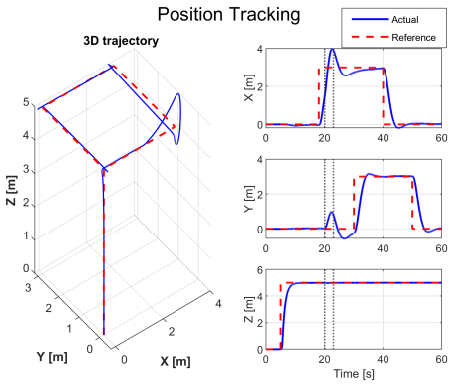

((a)) Position Tracking

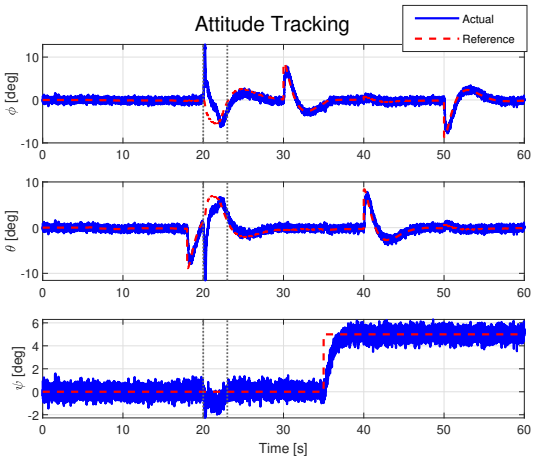

((b)) Attitude Tracking

Figure 5.5 : Motor 2 sudden LoE controller performance.

The third set of figures shows the response of the third motor during and after sudden LoF faults. Here the it can also be seen that the fault flag for Motor 3 is raised in a very short time, and the estimated fault magnitude aligns well with the actual loss.

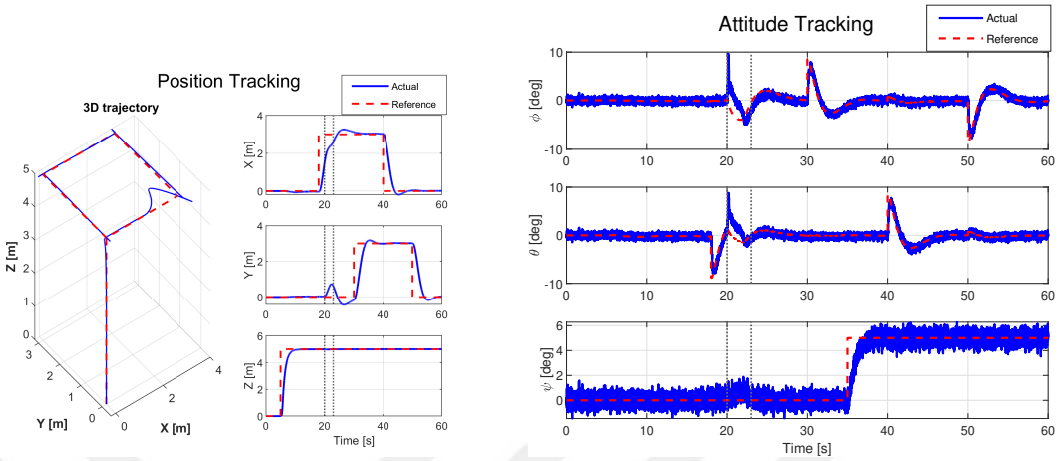

((a)) Position Tracking ((b)) Attitude Tracking

Figure 5.7 : Motor 3 sudden LoE controller performance.

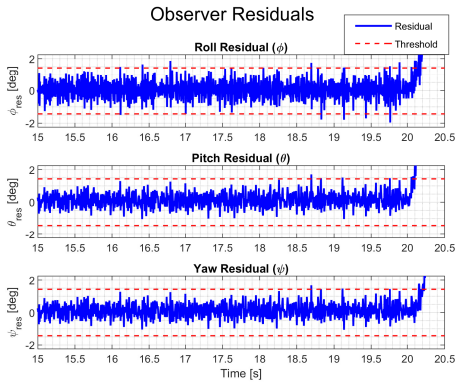

((a)) Residuals

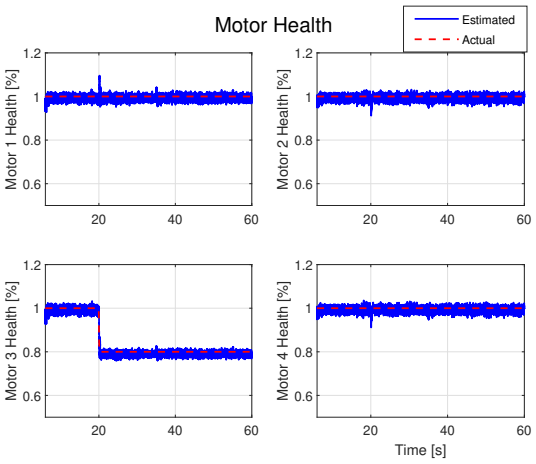

((b)) Motor Health

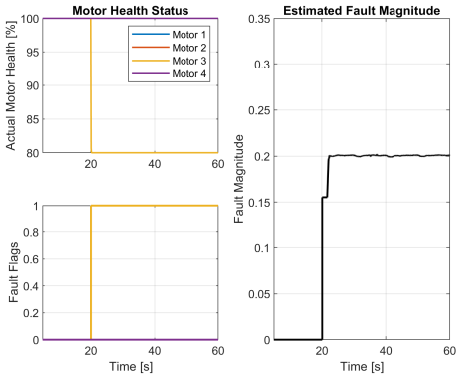

((c)) Motor fault flags and magnitude

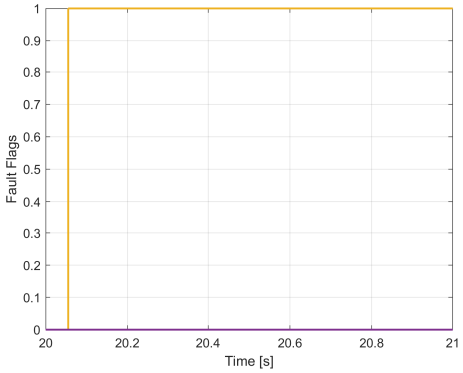

((d)) Fault flags

Figure 5.8 : Motor 3 sudden LoE FDI system performance.

The fourth set of figures shows the response of the fourth motor during and after sudden LoF faults. The results are almost the same as the other motors.

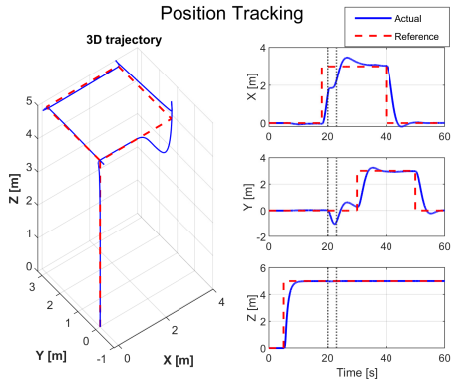

((a)) Position Tracking

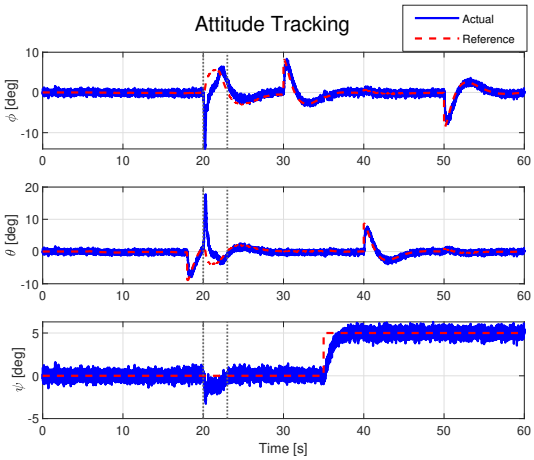

((b)) Attitude Tracking

Figure 5.9 : Motor 4 sudden LoE controller performance.

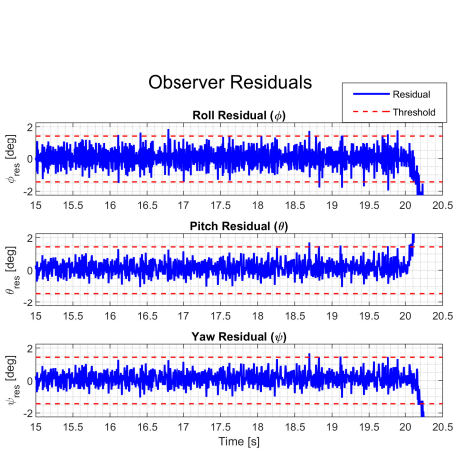

((a)) Residuals

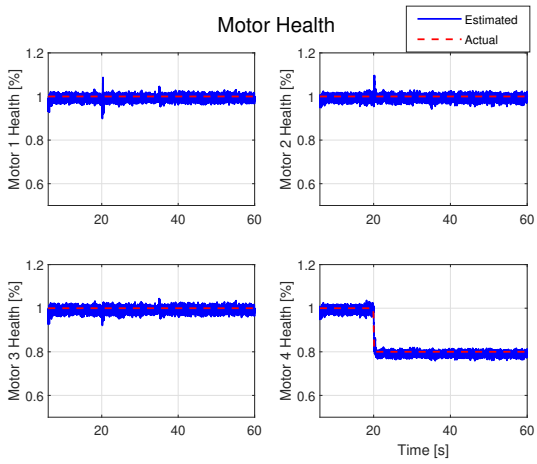

((b)) Motor Health

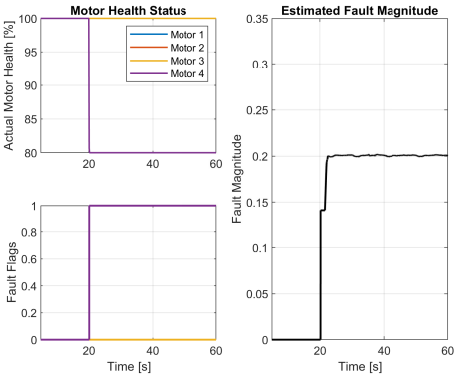

((c)) Motor fault flags and magnitude

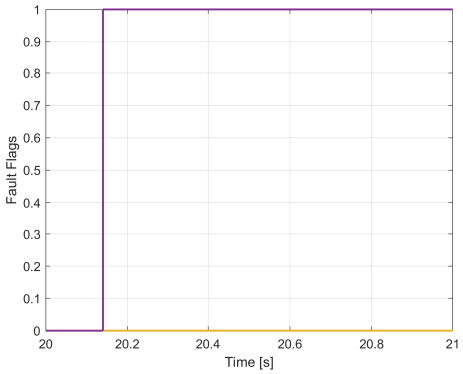

((d)) Fault flags

Figure 5.10 : Motor 4 sudden LoE FDI system performance.

The performance matrix evaluation of the faults yields a favorable result for the speed and robustness of the algorithms.

Table 5.3 : Sudden LoE performance evaluation metrics.

Performance	Motor 1	Motor 2	Motor 3	Motor 4
Detection Time[s]	0.14	0.11	0.1	0.14
False Alarm	0	0	0	0
Fault Magnitude Max Error [%]	1	1	1	1

5.3.4 Gradual loss of effectiveness (LOE)

Once the fault begins to occur, the residuals grow with the first progressive fault, and the fault is detected. The fault detection was within the same time windows as the sudden LOE case, while the estimation of fault magnitude followed the

true degradation trend with small error margins. Control stability was preserved, and the health-based control allocation adjusted motor commands effectively. The performance matrix evaluation for this case also yields promising results regarding the speed and robustness of the algorithms.

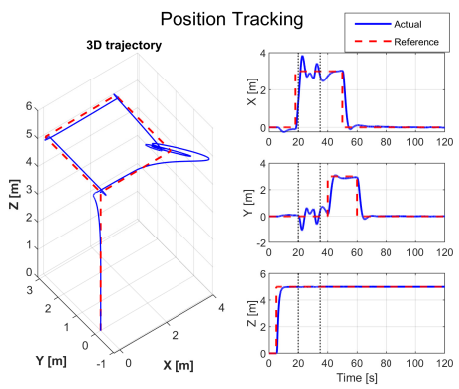

((a)) Position Tracking

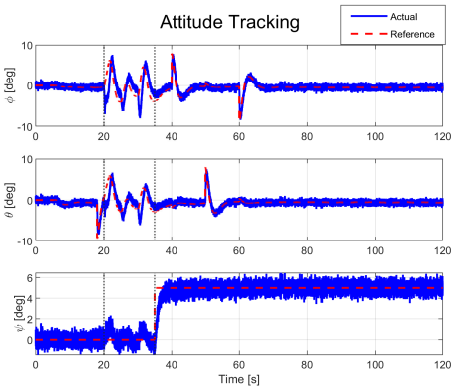

((b)) Attitude Tracking

Figure 5.11 : Motor 1 gradual LoE controller performance.

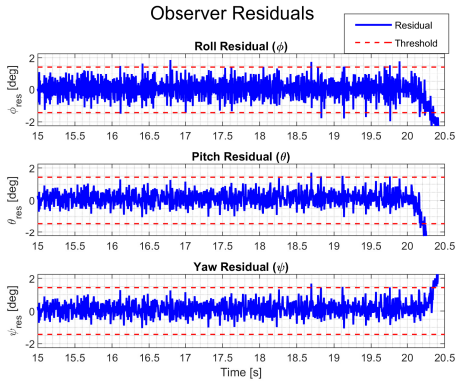

((a)) Residuals

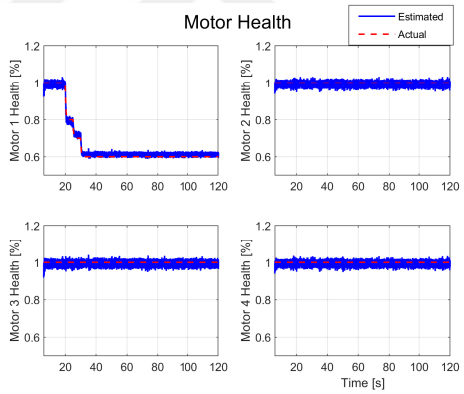

((b)) Motor Health

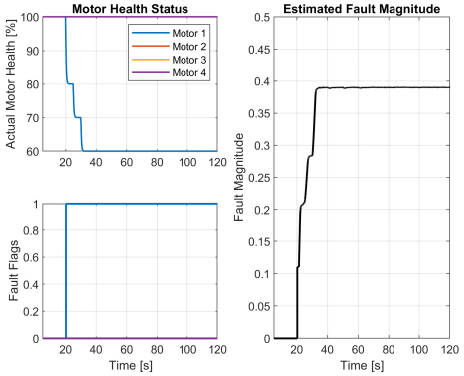

((c)) Motor fault flags and magnitude

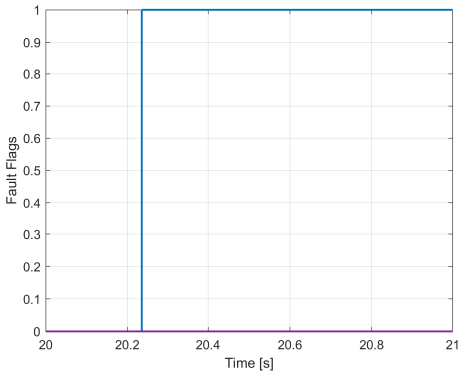

((d)) Fault flags

Figure 5.12 : Motor 1 gradual LoE FDI system performance.

In the first test, I applied a staged loss of effectiveness to the first motor, with the fault magnitude increasing from 10 percent to 40 percent in three steps. As the fault begins to occur, the Thau observer's residuals begin to exceed the thresholds and capture the first gradual fault. Meanwhile, the complementary observer estimates the motor health and effectively follows the gradual degradation.

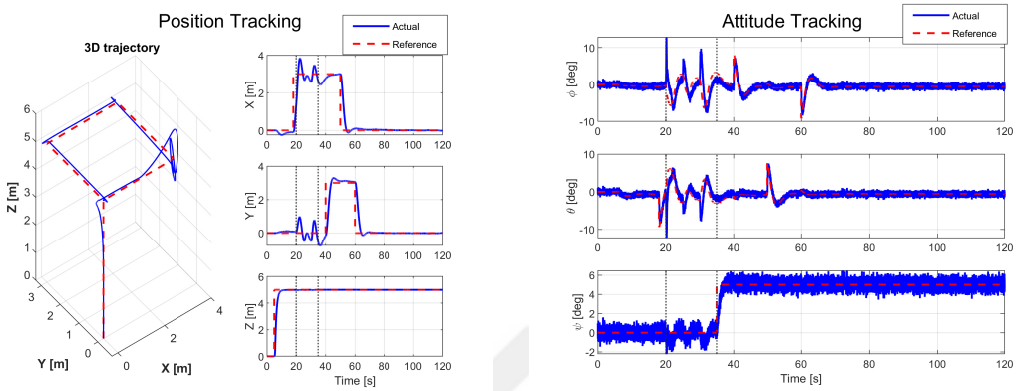

((a)) Position Tracking ((b)) Attitude Tracking

Figure 5.13 : Motor 1 gradual LoE controller performance.

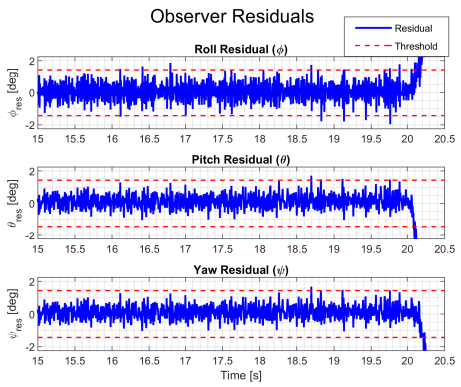

((a)) Residuals

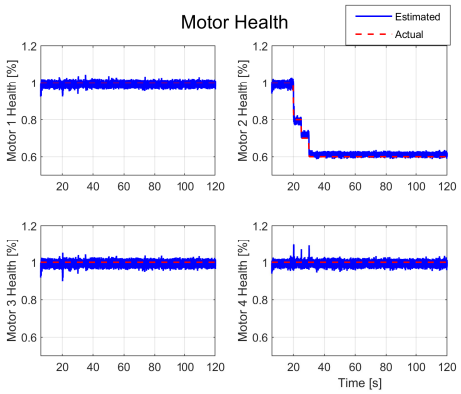

((b)) Motor Health

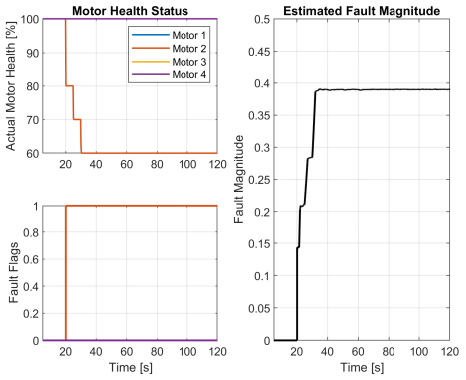

((c)) Motor fault flags and magnitude

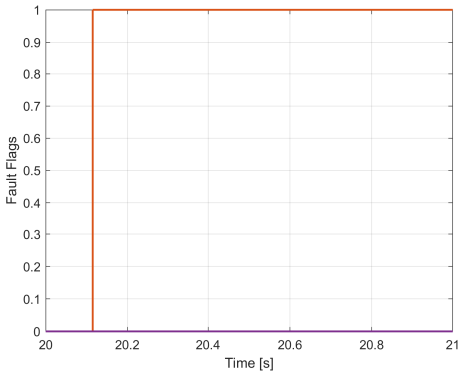

((d)) Fault flags

Figure 5.14 : Motor 2 gradual LoE FDI system performance.

In the second test, the same scenario is applied, and the system response is the same. The FDI system is detecting the motor errors without any false alarms.

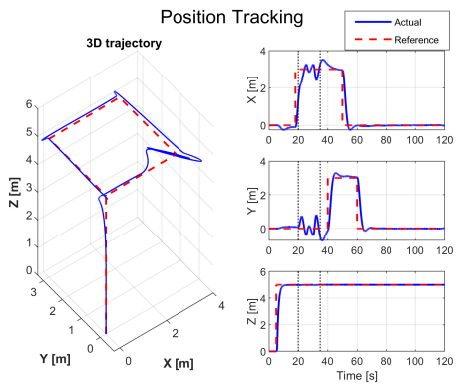

((a)) Position Tracking

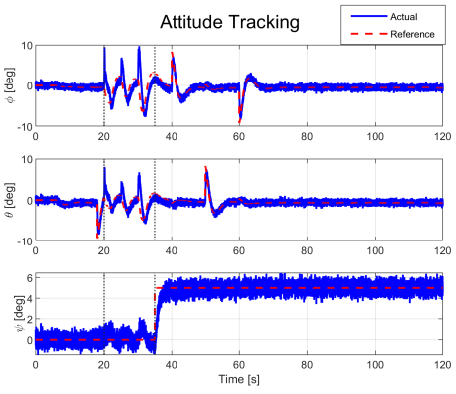

((b)) Attitude Tracking

Figure 5.15 : Motor 3 gradual LoE controller performance.

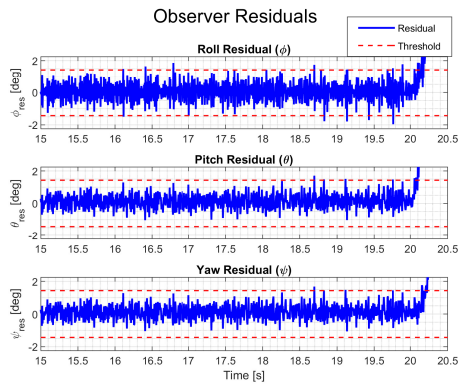

((a)) Residuals

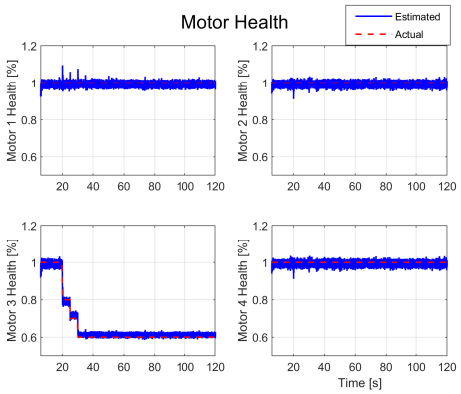

((b)) Motor Health

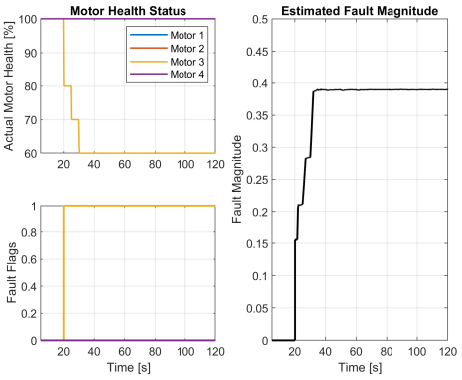

((c)) Motor fault flags and magnitude

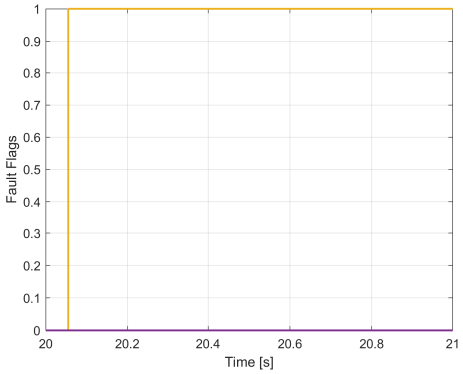

((d)) Fault flags

Figure 5.16 : Motor 3 gradual LoE FDI system performance.

The third motor test results are also the same. The FDI system succeeded in detecting the fault in approximately 0.1 seconds. The position and attitude of the aircraft are tracking the trajectories in a good manner.

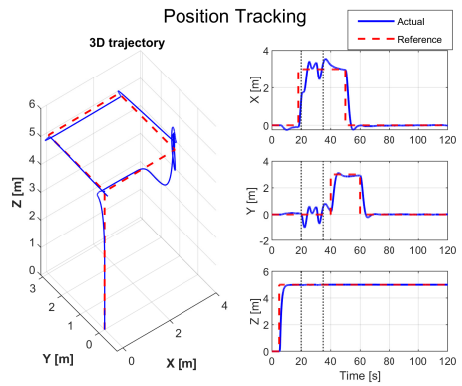

((a)) Position Tracking

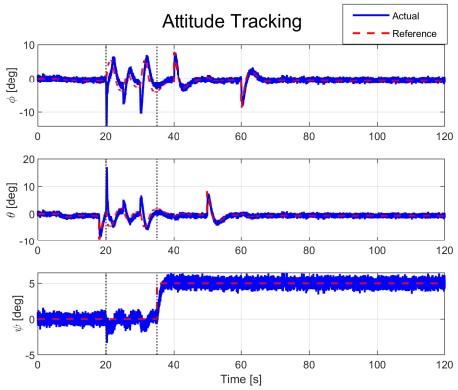

((b)) Attitude Tracking

Figure 5.17 : Motor 4 gradual LoE controller performance.

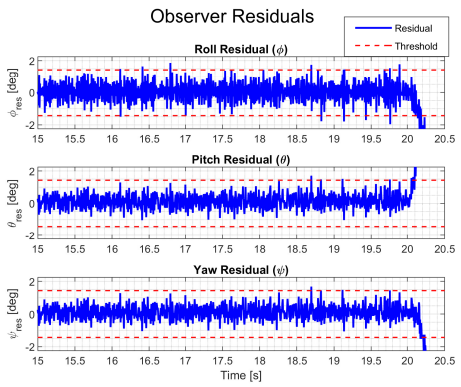

((a)) Residuals

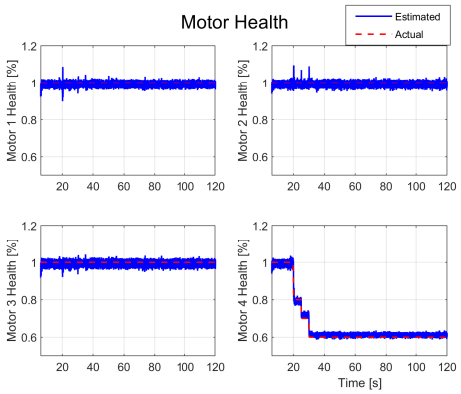

((b)) Motor Health

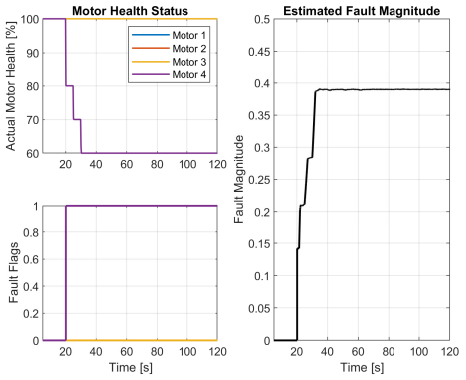

((c)) Motor fault flags and magnitude

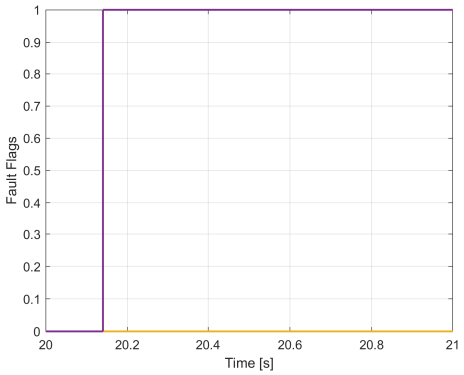

((d)) Fault flags

Figure 5.18 : Motor 4 gradual LoE FDI system performance.

Table 5.4 : Gradual LoE performance evaluation metrics.

Performance	Motor 1	Motor 2	Motor 3	Motor 4
Detection Time[s]	0.2	0.12	0.1	0.14
False Alarm	0	0	0	0
Fault Magnitude Max Error [%]	5	5	5	5

5.4 Discussion and Summary

The simulation results showed the effectiveness and robustness of the proposed FDI system in the presence of noise, external disturbance, and model errors. Across all scenarios, the nonlinear observer framework demonstrated reliable fault detection without compromising flight stability or triggering false positives. The dual-observer structure, consisting of the Thau observer and the dynamic inversion-based complementary observer, proved instrumental in separating state estimation from actuator monitoring.

Key observations include:

- The dynamic inversion-based observer enabled precise actuator health monitoring and facilitated real-time fault magnitude estimation.
- Adaptive thresholding strategies effectively balanced sensitivity and robustness under disturbances and sensor noise.
- Health-based control allocation tolerated actuator degradations and helped the controller sustain trajectory tracking under faulted conditions.

Regarding the gradual fault results, when a fault starts to occur in the system, the residuals from the observer initially stay within their expected range. However, as the fault gradually increases, the residuals exceed their threshold and begin to deviate further from their normal values. At this point, the observer's model can no longer accurately represent the system's dynamics because the fault is progressively affecting the system's behavior. Given that the residuals are no longer reliable after the fault is detected, the focus is shifted to a complementary observer, which is specifically designed to track the motor health. This complementary observer provides a more accurate representation of the fault's magnitude as it progresses over time, especially in cases of gradual faults. While the residuals become unreliable as the fault evolves, the complementary observer enables more effective monitoring of the fault's behavior and estimation of its magnitude. By relying on the complementary observer, I can continue

estimating the fault's progression and magnitude, ensuring that the system can adapt accordingly to maintain stability and performance, even as the fault gradually worsens.

6. CONCLUSIONS

6.1 Overview of the Study

This thesis focused on developing a robust Fault detection and isolation (FDI) system tailored for quad-rotors. The growing dependence on unmanned aerial vehicles in both civilian and critical applications underscores the importance of ensuring safe and reliable operation, especially under actuator degradation or external disturbances.

A model-based methodology was adopted. The system leveraged a nonlinear Thau observer to estimate the full state vector from available measurements and control inputs. Recognizing the limitations of purely state-based methods, a dynamic inversion-based complementary observer was also introduced to estimate actuator behavior by back-calculating motor speeds from body accelerations. This dual-observer architecture enabled the generation of two distinct types of residuals: one from state-tracking errors and another from actuator-level discrepancies.

The simulation environment built in MATLAB/Simulink closely reflected realistic flight conditions by incorporating sensor noise, actuator dynamics, and external disturbances. Multiple test scenarios were conducted, including nominal conditions as well as sudden and gradual loss-of-effectiveness (LOE) faults.

The results demonstrated:

- Accurate fault detection under various LOE conditions.
- Timely estimation of fault magnitude for control reallocation.
- Robustness to noise and initial estimation errors.
- Tolerance to faults through modified control allocation using health matrices.

All in all, this study really put the proposed Fault Detection and Isolation (FDI) strategy to the test in a simulation setup and showed it's both doable and practical.

It is considered a proof of concept that it could apply to small multi-rotor platforms, enhancing its reliability in real time. The work presented in this thesis offers some potential contributions to the field of fault detection in UAV systems:

- Robust Dual-Observer Strategy
- Fault Magnitude Estimation Mechanism
- Adaptive and Fault-Tolerant Control Allocation.
- Validated Performance Under Different Scenarios

These potential contributions collectively advance the reliability and autonomy of UAV platforms, offering a scalable solution that can be adapted to various multi-rotor configurations.

6.2 Limitations

The proposed FDI system has demonstrated promising performance. On the other hand, several limitations remain that should be acknowledged:

- **Single Fault Detection:** The current implementation is limited to detecting faults in only one motor at a time. Simultaneous multi-motor faults are not addressed.
- **Fault Type Restriction:** The system is designed to detect only actuator-related faults, specifically loss-of-effectiveness (LOE). Other types of faults, such as stuck-in-place or sensor faults, are not considered.
- **No Hardware Validation:** All evaluations are carried out in simulation. The transition to real-time hardware implementation may require further tuning and validation, especially in uncertain physical environments.

6.3 Future Work

Future work related to this topic could focus on addressing the key limitations and expanding the capabilities of the current system. Some potential directions include enhancing fault-tolerant control to include complete motor failure or to deal with other fault types, and enhancing the observer architecture to handle multiple simultaneous motor fault detection. Generalization to Other Fault Types: Extending the system to detect and classify a broader range of faults, such as intermittent failures, sensor degradation, or structural anomalies. Incorporating hybrid FDI strategies that combine model-based and data-driven methods may provide more comprehensive coverage. It can also include real-time Implementation, translating the proposed method to embedded hardware platforms for onboard execution in actual UAVs. This would involve real-time optimization, code generation, and experimental validation under real-world disturbances. These extensions aim to improve system autonomy, fault resilience, and practical deployment, ultimately enabling safer and more reliable UAV operation across diverse applications.

REFERENCES

[1] **Ducard, J.G.** (2009). *Fault-tolerant flight control and guidance systems: practical methods for unmanned aerial vehicles*, Springer.

[2] **Y. M. Zhang, A.C.** (2013). Development of advanced FDD and FTC techniques with application to an unmanned quadrotor helicopter testbed,, *Journal of the Franklin Institute*.

[3] **REN, X.L.** (2020). Observer Design for Actuator Failure of a Quadrotor,, *IEEE*.

[4] **Mulgundkar, A.** (2023). *Actuator Fault Detection, Isolation and Fault Tolerant Control of A Hexacopter UAV*.

[5] **Hocaoglu, Y.** (2021). *Fault Tolerant Control of a Quadrotor Helicopter,*.

[6] **Ranjbaranhesarmaskan, M.** (2010). *Fault Recovery of an Under-Actuated Quadrotor Aerial Vehicle,*.

[7] **A. Freddi, S.L. and Monteriu, A.** (2012). Actuator Fault Detection System for a Mini-Quadrotor, *Journal of Intelligent Robotic Systems*.

[8] **A. Freddi, S.L. and Monteriu, A.** (2010). Actuator Fault Detection System for a Mini-Quadrotor, *2010 IEEE International Symposium on Industrial Electronics*.

[9] **Guzma´n-Rabasa1, Francisco Ronay, B.C.G.V.P.M.C. and Pe´rez-Patricio, M.** (2019). Actuator fault detection and isolation on a quadrotor unmanned aerial vehicle, *Sage Journal*.

[10] **M. Saied, B. Lussier, I.F.H.S. and Francis, C.** (2017). Fault Diagnosis and Fault-Tolerant Control of an Octorotor UAV using motors speeds measurements, *20th International Federation of Automatic Control World Congress*.

[11] **R. Puchalski, A. Bondyra, W.G. and Zhang, Y.** (2022). Actuator fault detection and isolation system for multirotor unmanned aerial vehicles, *26th International Conference on Methods and Models in Automation*.

[12] **Ahmed Khattab, Halim Alwi, C.E.** (2019). Mitigating total rotor failure in quadrotor using LPV based sliding mode control scheme, *4th Conference on Control and Fault Tolerant Systems,*, Morocco.

CURRICULUM VITAE

Muhammed ARSLAN:

EDUCATION:

- **B.Sc.:** 2020, Istanbul Technical University, Aeronautical Engineering, Aeronautical and Astronautical Department

PROFESSIONAL EXPERIENCE AND REWARDS:

- 2020-present Baykar Technology.

PUBLICATIONS, PRESENTATIONS AND PATENTS ON THE THESIS:

- **ARSLAN M.**, INALHAN G. (2025). Quadrotor Actuator Fault Detection and Isolation. Model-Based Approach. *4th International Graduate Research Symposium*, May 12-14, 2025, Istanbul, Turkey. (Presentation Instance)